Laboratory of Analytical Chemistry
Department of Chemistry
University of Helsinki
Finland

Miniaturized mass spectrometric ionization techniques for environmental analysis and bioanalysis

Laura Luosujärvi

Academic Dissertation

To be presented, with the permission of
the Faculty of Science of the University of Helsinki,
for public criticism in Auditorium A110 of the Department of Chemistry
(A.I. Virtasen aukio 1, Helsinki)
on June 11th, 2010, at 12 o'clock noon.

Supervisors	Prof. Tapio Kotiaho Laboratory of Analytical Chemistry Department of Chemistry Faculty of Science and Division of Pharmaceutical Chemistry Faculty of Pharmacy University of Helsinki
	Prof. Risto Kostiainen Division of Pharmaceutical Chemistry Faculty of Pharmacy University of Helsinki
	Doc. Tiina Kauppila Division of Pharmaceutical Chemistry Faculty of Pharmacy University of Helsinki
Reviewers	Prof. Seppo Auriola School of Pharmacy Faculty of Health Sciences University of Eastern Finland
	Prof. Kimmo Peltonen Chemistry and Toxicology Research Unit Evira (Finnish Food Safety Authority)
Opponent	Prof. Jörg Kutter DTU Nanotech Department of Micro- and Nanotechnology Technical University of Denmark

ISBN 978-952-92-7362-1 (paperback)
ISBN 978-952-10-6286-5 (PDF)
http://ethesis.helsinki.fi

Helsinki University Print
Helsinki 2010

Contents

Preface

This thesis is based on research carried out in the Laboratory of Analytical Chemistry and the Division of Pharmaceutical Chemistry at the University of Helsinki during the years 2005-2010. Funding was provided by the Graduate School of Chemical Sensors and Microanalytical Systems (CHEMSEM) and the Finnish Funding Agency for Technology and Innovation (Tekes).

I am most grateful to my supervisors, Professors Tapio Kotiaho and Risto Kostiainen, and Docent Tiina Kauppila, for their encouragement, patience, fresh ideas and positive attitude. Without them the work would have never been completed. Warm thanks go to my co-authors for their valuable contributions, especially to Markus Haapala for his help in the laboratory and to Ville Saarela for manufacturing the microchips. Thanks, too, to Professors Seppo Auriola and Kimmo Peltonen, who carried out a careful review of this manuscript and provided valuable comments for its improvement.

I am indebted to past and present personnel of the laboratories for astute advice, technical assistance, and the creation of a pleasant working atmosphere, and to the team at the Department of Micro and Nanosciences at the Aalto University School of Science and Technology for fruitful collaboration.

Many good friends have helped me along the way: friends from school and at the University of Jyväskylä, whose friendships have lasted in spite of long distances, and friends in the Polyteknikkojen Orkesteri. Special thanks go to Michael for his encouragement and support, my sister Maria for always being at my side, and my parents Kaija and Erkki for their confidence in me and endless support in all possible ways.

Helsinki, May 2010

Laura Luosujärvi

Abstract

Novel miniaturized mass spectrometric ionization techniques based on atmospheric pressure chemical ionization (APCI) and atmospheric pressure photoionization (APPI) were studied and evaluated in the analysis of environmental samples and biosamples. The three analytical systems investigated here were gas chromatography-microchip atmospheric pressure chemical ionization-mass spectrometry (GC-μAPCI-MS) and gas chromatography-microchip atmospheric pressure photoionization-mass spectrometry (GC-μAPPI-MS), where sample pretreatment and chromatographic separation precede ionization, and desorption atmospheric pressure photoionization-mass spectrometry (DAPPI-MS), where samples are analyzed either as such or after minimal pretreatment.

The gas chromatography-microchip atmospheric pressure ionization-mass spectrometry (GC-μAPI-MS) instrumentations were used in the analysis of polychlorinated biphenyls (PCBs) in negative ion mode and 2-quinolinone-derived selective androgen receptor modulators (SARMs) in positive ion mode. The analytical characteristics (i.e., limits of detection, linear ranges, and repeatabilities) of the methods were evaluated with PCB standards and SARMs in urine. All methods showed good analytical characteristics and potential for quantitative environmental analysis or bioanalysis.

Desorption and ionization mechanisms in DAPPI were studied. Desorption was found to be a thermal process, with the efficiency strongly depending on thermal conductivity of the sampling surface. Probably the size and polarity of the analyte also play a role. In positive ion mode, the ionization is dependent on the ionization energy and proton affinity of the analyte and the spray solvent, while in negative ion mode the ionization mechanism is determined by the electron affinity and gas-phase acidity of the analyte and the spray solvent. DAPPI-MS was tested in the fast screening analysis of environmental, food, and forensic samples, and the results demonstrated the feasibility of DAPPI-MS for rapid screening analysis of authentic samples.

List of original publications

This thesis is based on the papers listed below, hereafter referred to by their Roman numerals (**I-V**).

I Laura Luosujärvi, Mika-Matti Karikko, Markus Haapala, Ville Saarela, Sami Huhtala, Sami Franssila, Risto Kostiainen, Tapio Kotiaho, Tiina J. Kauppila: Gas chromatography/mass spectrometry of polychlorinated biphenyls using atmospheric pressure chemical ionization and atmospheric pressure photoionization microchips, *Rapid Commun. Mass Spectrom.*, 22(4) (2008) 425-431.

II Laura Luosujärvi, Markus Haapala, Mario Thevis, Ville Saarela, Sami Franssila, Raimo A. Ketola, Risto Kostiainen, Tapio Kotiaho: Analysis of selective androgen receptor modulators by gas chromatography-microchip atmospheric pressure photoionization-mass spectrometry, *J. Am. Soc. Mass Spectrom.*, 21(2) (2010) 310-316.

III Laura Luosujärvi, Ville Arvola, Markus Haapala, Jaroslav Pól, Ville Saarela, Sami Franssila, Tapio Kotiaho, Risto Kostiainen, Tiina J. Kauppila: Desorption and ionization mechanisms in desorption atmospheric pressure photoionization, *Anal. Chem.*, 80(19) (2008) 7460-7466.

IV Laura Luosujärvi, Sanna Kanerva, Ville Saarela, Sami Franssila, Risto Kostiainen, Tapio Kotiaho, Tiina J. Kauppila: Environmental and food analysis by desorption atmospheric pressure photoionization-mass spectrometry, *Rapid Commun. Mass Spectrom.*, 24(9) (2010) 1343-1350.

V Laura Luosujärvi, Ulla-Maija Laakkonen, Risto Kostiainen, Tapio Kotiaho, Tiina J. Kauppila: Analysis of street market confiscated drugs by desorption atmospheric pressure photoionization and desorption electrospray ionization coupled with mass spectrometry, *Rapid Commun. Mass Spectrom.*, 23(9) (2009) 1401-1404.

The contribution of the author:

Paper I: The experimental work was planned by the author with contributions from the others. The experimental work was carried out by the author and Mika-Matti Karikko except for the microfabrication, the soil sample extraction, and the GC-ECD analysis. The article was written by the author with contributions from the others.

Paper II: The experimental work was planned by the author, and, except for the microfabrication, the SARM synthesis, and the GC-EI-MS analysis, carried out by the author with contributions from Markus Haapala. The article was written by the author with contributions from the others.

Paper III: The experimental work was planned by Doc. Tiina J. Kauppila and the author. The experimental work was carried out by the author, with contributions from Markus Haapala and Ville Arvola, except for the microfabrication. The article was written by the author with contributions from the others.

Paper IV: The experimental work was planned and carried out by the author, except for the microfabrication and the preparation of the soil pellets. The article was written by the author with contributions from the others.

Paper V: The experimental work was planned and carried out by the author, except for the microfabrication and the GC and LC analyses. The article was written by the author with contributions from the others.

Abbreviations and symbols

APCI	atmospheric pressure chemical ionization
APGDDI	atmospheric pressure glow discharge desorption/ionization
API	atmospheric pressure ionization
APPI	atmospheric pressure photoionization
BaP	benzo[a]pyrene
BkF	benzo[k]fluoranthene
BRF	brominated flame retardant
CI	chemical ionization
DAPPI	desorption atmospheric pressure photoionization
DESI	desorption electrospray ionization
D/I	desorption/ionization
EA	electron affinity
ECD	electron capture detector
EI	electron ionization
EIC	extracted ion chromatogram
ESI	electrospray ionization
FID	flame ionization detector
GC	gas chromatography or gas chromatograph
h	Planck constant
IE	ionization energy
ISTD	internal standard
LOD	limit of detection
LOQ	limit of quantitation
MDMA	3,4-methylenedioxymethamphetamine
MS	mass spectrometry or mass spectrometer
MS/MS	tandem mass spectrometry
m/z	mass-to-charge ratio
ν	frequency
PA	proton affinity
PAH	polycyclic aromatic hydrocarbon
PBDE	polybrominated diphenyl ether
PCB	polychlorinated biphenyl
PMMA	poly(methyl methacrylate)
PTFE	poly(tetrafluoroethylene)
RPLC	reversed phase liquid chromatography
RSD	relative standard deviation
SARM	selective androgen receptor modulator
SRM	selected reaction monitoring
SSI	sonic spray ionization
TBBPA	tetrabromobisphenol A
UV	ultra violet

1 Introduction

The miniaturization of analytical devices has gained much interest in recent years [1-4]. The advantages of miniaturized devices over conventional systems include higher separation efficiency and faster analysis consequent upon the shorter reaction times. The consumption of samples, reagents, and solvents is drastically decreased, which translates into lower operating costs and less chemical waste. The possibility of mass production of miniaturized devices by microfabrication processes promises low unit costs, enabling the manufacturing of disposable devices. And eventually, the smaller size and reduced need for chemicals and electrical power may allow the manufacturing of portable, high sensitivity systems.

Mass spectrometry (MS) is a powerful tool for analytical applications thanks to its capability to detect trace amounts of analytes in complex mixtures. Until now, the main object of miniaturization in mass spectrometric analytical devices has been the ion source. Miniaturized ion sources have been introduced for electrospray ionization (ESI), atmospheric pressure chemical ionization (APCI), and atmospheric pressure photoionization (APPI), and all three can be used to couple a gas chromatograph (GC) or a liquid chromatograph (LC) with any mass spectrometer (MS) equipped with an atmospheric pressure ionization (API) interface. Miniaturized ionization techniques are relatively new, however, and much work remains to be done. More stable operation and more reliable analytics need to be achieved, and analytical applications are needed to demonstrate the feasibility of the miniaturized ionization techniques in real-life analysis, such as environmental analysis and bioanalysis.

In addition to miniaturized ionization techniques, much effort has gone into the development of “ambient desorption/ionization” [5] or “atmospheric pressure surface sampling” [6] techniques, including desorption electrospray ionization (DESI) [7] and desorption atmospheric pressure photoionization (DAPPI) [8]. In ambient desorption/ionization techniques the analytes are desorbed directly from sample surfaces and immediately ionized. Ambient desorption/ionization methods are characterized by minimal sample pre-treatment, or even no pretreatment at all, and by analysis times as short as seconds per sample, enabling faster overall analysis. As with the other novel ionization approaches, further study and development of the ambient desorption/ionization techniques is needed to obtain more reliable and useful analytics.

A myriad of harmful organic compounds have been flushed into the environment since the advent of industrialization [9]. A great many of these compounds are now under scrutiny for their possible adverse health effects [10-14]. Chemical determinations of compounds such as polychlorinated biphenyls (PCBs), polycyclic aromatic hydrocarbons (PAHs), and pesticides in environmental samples are needed to estimate the risk that these compounds pose to humans and wildlife, and to support decision-making about protection and legislation. In addition, chemical analysis is widely needed in bioanalytical applications such as diagnosis and monitoring of diseases [15], doping control [16], and drug discovery [17]. Among the compounds of interest in bioanalysis are hormones and licit and illicit drugs and their metabolites. The sample matrices in environmental analysis and bioanalysis – soil, plant parts, biological fluids – are typically complex and since they usually interfere with the actual analysis, sample preparation to remove interfering compounds plays a key role in the analytical process. Effective separation of the compounds of interest from the sample matrix requires various time-consuming sample

preparation stages such as sifting, grinding, hydrolysis, extraction, and derivatization. After pretreatment the target compounds in a sample are typically separated by GC or LC, and detected by MS. Despite recent advances in sample pretreatment [18] the pretreatment stage often remains the bottleneck in the whole analytical process. Thus, any technique that does not require extensive sample preparation will speed up the analytical process markedly.

The research presented in this thesis exploits novel mass spectrometric ionization techniques in environmental analysis and bioanalysis. The analytical performance of gas chromatography-microchip atmospheric pressure chemical ionization-mass spectrometry (GC-µAPCI-MS) and gas chromatography-microchip atmospheric pressure photoionization-mass spectrometry (GC-µAPPI-MS) was evaluated, and the applicability of these techniques in environmental analysis (**I**) and bioanalysis (**II**) was tested. Analysis of PCBs in soil was performed with an ion trap MS in negative ion mode (**I**), and selected androgen receptor modulators (SARMs) in urine were analyzed with a triple quadrupole MS operating in positive ion mode (**II**). Direct analysis of samples, without sample preparation, was carried out with an ambient desorption/ionization technique, DAPPI. After study of the desorption and ionization mechanisms in DAPPI, and optimization of the geometry of the DAPPI ion source (**III**), compounds in environmental or food matrices (**IV**) and in illicit drug powders (**V**) were analyzed by DAPPI-MS. For comparison of the performance of the ambient desorption/ionization methods, the illicit drugs were also analyzed by DESI-MS (**V**).

Chapter 2 reviews the most widely used atmospheric pressure ionization techniques, while Chapter 3 describes present mass spectrometric methods for environmental analysis and bioanalysis. The aims of the study and the experimental details are summarized in Chapters 4 and 5, respectively. The results of analyses carried out with GC-µAPCI-MS and GC-µAPPI-MS are discussed in the first part of Chapter 6 (section 6.1), and the DAPPI-MS results in the second part (section 6.2). Chapter 7 summarizes the findings of the study and offers conclusions.

2 Atmospheric pressure ionization techniques for mass spectrometry

A multitude of API techniques for MS have been developed during the last decades [19]. A common feature of these techniques is the formation of intact ions such as protonated or deprotonated molecules. Nowadays, the most popular API techniques are electrospray ionization (ESI) [20,21] together with its modification ionspray [22], APCI [23,24], and APPI [25,26]. This chapter reviews the ionization mechanisms in API and the recently introduced miniaturized spray ionization techniques and ambient desorption/ionization techniques.

2.1 Ionization mechanisms in atmospheric pressure ionization

The ionization mechanisms in ESI, APCI, and APPI are discussed below together with simplified ionization reactions in APCI and APPI.

Electrospray ionization

In ESI, high voltage, 3–5 kV, is connected to the electrospray capillary while the mass spectrometer MS interface is grounded, or vice versa [27]. The strong electric field causes the liquid sample to ionize, and it forms a fine mist of charged droplets as it exits the ESI sprayer tip. The charged droplets shrink due to solvent evaporation and droplet fission, and gas-phase ions are formed. Typically, ionization occurs by protonation ($[M+H]^+$) in positive ion mode, by deprotonation ($[M-H]^-$) in negative ion mode, or by adduct formation (for example, $[M+Na]^+$, $[M+NH_4]^+$, or $[M+Cl]^-$) in both positive and negative ion modes. ESI is ideal for analytes of moderately polar to polar character. It is considered as a soft ionization technique and thus also suitable for thermolabile and large molecules with masses up to 100 000 u, such as large biomolecules [28]. The main use of ESI is in coupling of LC to MS [29].

Atmospheric pressure chemical ionization

In APCI, the sample solution is vaporized by heated pneumatic nebulizer and the analytes are ionized in gas phase by corona discharge. The ionization reaction mechanisms presented below have been presented by Carroll et al. [30] for positive APCI and by Dzidic et al. [31,32] for negative APCI.

In positive ion APCI, the primary ions are formed from atmospheric gases (reactions 1 and 2). The electrons taking part in initial reactions (reaction 1) are free electrons from the air, which are accelerated in the electric field between the corona needle electrode and the ground electrode. The primary ions collide with atmospheric water molecules (reactions 3-5) to form protonated reactant ions ($H^+(H_2O)_n$, $n \geq 1$). If the proton affinity of the analyte is higher than that of the water cluster, the gas-phase analyte is ionized in proton transfer reaction with the protonated water cluster to form protonated analyte molecule ($[M+H]^+$) (reaction 6).

1 $N_2 + e^- \rightarrow N_2^{+\bullet} \xrightarrow{N_2/O_2} N_4^{+\bullet} \xrightarrow{O_2} O_2^{+\bullet}$

2 $O_2 + e^- \rightarrow O_2^{+\bullet} \xrightarrow{O_2} O_4^{+\bullet}$

3 $O_2^{+\bullet} + H_2O \rightarrow O_2^{+\bullet}(H_2O)$ also with $O_4^{+\bullet}$

4 $O_2^{+\bullet}(H_2O) + H_2O \rightarrow O_2^{+\bullet}(H_2O)_2 \rightarrow H_3O^{+\bullet}(OH) + O_2$

5 $H_3O^{+\bullet}(OH) + H_2O_{(n-1)} \rightarrow H^+(H_2O)_n + OH^\bullet$

6 $M + H^+(H_2O)_n \rightarrow [M+H]^+ + (H_2O)_n$ if PA(M) > PA($(H_2O)_n$)

If solvent (LC solvent) is present in the system, the protonated water clusters react with the solvent molecules or solvent clusters (S_m, $m \geq 1$) through proton transfer (reaction 7) to form protonated solvent species ($S_mH^+(H_2O)_n$). Proton transfer reaction between the analytes and the protonated solvent species leads to the formation of protonated analyte molecules ($[M+H]^+$) (reaction 8). If solvent with low IE is used, formation of radical cations ($S^{+\bullet}$) from the solvent can occur either by direct ionization (reaction 9) or by charge exchange with primary ions (reaction 10). Solvent radical cations ($S^{+\bullet}$) will react with analyte to produce analyte radical cations ($M^{+\bullet}$) (reaction 11) if the IE of the analyte is lower than that of the solvent. However, protonated solvent species are formed with the most popular LC solvents, water/methanol and water/acetonitrile.

7 $S_m + H^+(H_2O)_n \rightarrow S_mH^+(H_2O)_n$ if PA(S_m) > PA($(H_2O)_n$)

8 $M + S_mH^+(H_2O)_n \rightarrow [M+H]^+ + S_m(H_2O)_n$ if PA(M) > PA($S_m(H_2O)_n$)

9 $S + e^- \rightarrow S^{+\bullet} + 2e^-$

10 $S + O_2^{+\bullet} \rightarrow S^{+\bullet} + O_2$

11 $M + S^{+\bullet} \rightarrow M^{+\bullet} + S$ if IE(M) < IE(S)

In negative ion APCI, atmospheric oxygen plays an important role in reactant ion formation. Since O_2 has positive electron affinity (EA) (0.45 eV [33]), oxygen forms superoxide ions ($O_2^{-\bullet}$) by electron capture (reaction 12). If the EA of the analyte is greater than that of O_2, superoxide ions can react with the analytes by charge exchange, which leads to the formation of negative molecular ions ($M^{-\bullet}$) (reaction 13). If the analyte possesses positive EA, $M^{-\bullet}$ ions can also form by electron capture (reaction 14). In addition, if the gas-phase acidity of the analyte is greater than that of the hydroperoxy radical ($HO_2^\bullet$), superoxide ion may react with the analyte through proton transfer (reaction 15), leading to the formation of deprotonated analyte molecule ($[M-H]^-$). In addition to the $M^{-\bullet}$ and $[M-H]^-$ ions, phenoxide ions ($[M-X-O]^-$, where X is for example Cl or H) may form from substituted aromatic compounds [32,34-36] (reactions 16 and 17).

12 $O_2 + e^- \rightarrow O_2^{-\bullet}$

13 $M + O_2^{-\bullet} \rightarrow M^{-\bullet} + O$ if EA(M) > EA(O_2)

14 $M + e^- \rightarrow M^{-\bullet}$ if EA(M) > 0 eV

15 $M + O_2^{-\bullet} \rightarrow [M-H]^- + HO_2^\bullet$ if ΔG_{acid} (M) < ΔG_{acid} ($HO_2^\bullet$)

16 $M + O_2^{-\bullet} \rightarrow [M - X + O]^- + OX^\bullet$ X: for example Cl or H

17 $M^{-\bullet} + O_2 \rightarrow [M - X + O]^- + OX^\bullet$

If solvent is added to the system, deprotonation of the solvent or solvent cluster (S_m, $m \geq 1$) may occur in a reaction with superoxide ion ($O_2^{-\bullet}$) if the gas-phase acidity of S_m is higher than that of the hydroperoxy radical ($HO_2^\bullet$). In such a case deprotonated solvent species ($[S_m\text{-}H]^-$) are formed (reaction 18). Deprotonated analyte molecule can form in proton transfer reaction with $[S_m\text{-}H]^-$ (reaction 19) if the gas-phase acidity of the analyte is higher than that of the solvent cluster (S_m). However, the ΔG_{acid} values of the most used LC solvents are higher than that of hydroperoxy radical (ΔG_{acid} for acetonitrile: 1528 kJ/mol, methanol: 1565 kJ/mol, water: 1607 kJ/mol, and hydroperoxy radical: 1451 kJ/mol [33]), and thus reaction 18 does not occur when using those solvents. Instead, acidic analytes can form deprotonated molecules ($[M\text{-}H]^-$) through proton transfer reaction with superoxide ion (reaction 15) or some other reactant ion.

18 $S_m + O_2^{-\bullet} \rightarrow [S_m - H]^- + HO_2^\bullet$ if $\Delta G_{acid}(S_m) < \Delta G_{acid}(HO_2^\bullet)$

19 $M + [S_m - H]^- \rightarrow [M - H]^- + S_m$ if $\Delta G_{acid}(M) < \Delta G_{acid}(S_m)$

Since APCI includes thermal evaporation, the analytes need to be thermally stable. In general, the ionization conditions are considered harder than those in ESI. In combination with LC, APCI tolerates higher buffer concentrations than ESI and, in addition, both polar and nonpolar solvents can be used in APCI, whereas ESI allows only polar and medium polar solvents. APCI is more sensitive to ionic – acidic or basic – compounds in their neutral form than ionic form. This feature is an advantage when using reversed phase LC-MS (RPLC-MS), where the analytes are better retained to non-polar solid phase in their neutral form than in their ionic form. In contrast, ESI has better sensitivity to ionic species. Thus APCI is a favorable ionization method over ESI when acidic or basic compounds are analyzed by RPLC-MS. Importantly, APCI is suitable for gaseous samples, too, and can be utilized in coupling of both LC and GC to MS [37,38]. The main use is in LC-MS, however [29].

Atmospheric pressure photoionization

Sample introduction in APPI is similar to that in APCI (vaporization by heated pneumatic nebulizer), but the ionization is initiated by energetic photons instead of corona discharge. The following APPI reaction mechanisms are presented by Hanold et al. (positive ion mode [39]) and Kauppila et al. (positive [40] and negative [36] ion modes).

Direct photoionization of a gas-phase analyte (M) may occur if the IE of the analyte is lower than the energy of the photon ($h\nu$, where h is the Planck constant and ν is the frequency of the photon) (reaction 20).

20 $M + h\nu \rightarrow M^{+\bullet} + e^-$ if $IE(M) < h\nu$

However, dopant-assisted photoionization, where an easily ionizable organic solvent is added to the ion source, is often exploited in APPI. The purpose of the solvent, dopant (D), is to act as charge carrier and enhance the photoionization. Toluene is a suitable dopant since its IE (8.8 eV [33]) is below the energy of the photons emitted by commonly used UV lamps (usually 10 eV). The dopant is vaporized together with the solvent and sample, and ionized by photons to form radical cations ($D^{+\bullet}$) (reaction 21). If the ionization energy of the analyte is lower than that of the dopant, $D^{+\bullet}$ ions react further

through charge exchange with the analytes (M) to produce analyte molecular ions ($M^{+\bullet}$) (reaction 22). Some dopants, acetone for example, undergo self-protonation to form protonated species ($[D_n+H]^+$) from the dopant radical cations and dopant clusters (reaction 23) [41,42]. If the PA of the analyte is higher than that of the dopant cluster, the analytes are ionized by proton transfer to form protonated analyte molecules ($[M+H]^+$) (reaction 24).

21 $D + h\nu \rightarrow D^{+\bullet} + e^-$ if IE(D) < hν

22 $M + D^{+\bullet} \rightarrow M^{+\bullet} + D$ if IE(M) < IE(D)

23 $D^{+\bullet} + D_n \rightarrow [D_n + H]^+ + [D - H]^\bullet$

24 $M + [D_n + H]^+ \rightarrow [M + H]^+ + D_n$ if PA(M) > PA(D_n)

Similar ionization reactions to those in dopant-assisted APPI may occur in dopant-free APPI when an LC solvent is present. If the IE of the solvent is below the energy of the photons (hν), the solvent (S) can undergo direct photoionization to form radical cations ($S^{+\bullet}$) (reaction 25). And if the IE of the analyte (M) is lower than that of the solvent, $S^{+\bullet}$ ion will react further with analyte (reaction 26), as in the reaction of $D^{+\bullet}$ ion with the analyte, leading to the formation of molecular ions ($M^{+\bullet}$). Some solvents, such as 2-propanol, form radical cations, which react further by self-protonation as in the reaction presented for a dopant (reaction 23), and form protonated solvent clusters ($[S_n+H]^+$]) (reaction 27). If the PA of the analyte is greater than that of the solvent cluster, the analyte will react with the protonated solvent cluster (reaction 28) to form protonated analyte molecules ($[M+H]^+$).

25 $S + h\nu \rightarrow S^{+\bullet} + e^-$ if IE(S) < hν

26 $M + S^{+\bullet} \rightarrow M^{+\bullet} + S$ if IE(M) < IE(S)

27 $S^{+\bullet} + S_m \rightarrow [S_m + H]^+ + [S - H]^\bullet$

28 $M + [S_m + H]^+ \rightarrow [M + H]^+ + S_m$ if PA(M) > PA(S_m)

Introduction of dopant and LC solvent simultaneously to an APPI ion source alters the ionization reactions. If the PA of the solvent is higher than that of the deprotonated dopant radical $[D\text{-}H]^\bullet$, radical cation formed from the dopant can react through proton transfer with the solvent to produce a protonated solvent cluster ($[S_m+H]^+$, $m \geq 1$) (reaction 29). Neutralization of the dopant radical cation (reaction 29) inhibits the analyte ionization through charge exchange (reaction 22). However, when a dopant with relatively high PA, such as anisole, is used, the dopant radical cations ($D^{+\bullet}$) are retained, and analyte radical cations ($M^{+\bullet}$) may form (reaction 22). If the proton affinity of the analyte is greater than that of the solvent, protonated solvent clusters ($[S_n+H]^+$) will react with analytes to form protonated analyte molecules ($[M+H]^+$) (reaction 30). Protonated analyte molecules, $[M+H]^+$, can also form by hydrogen abstraction from a protic solvent, such as methanol, to the analyte radical cation (reaction 31).

29 $S_m + D^{+\bullet} \rightarrow [S_m + H]^+ + [D - H]^\bullet$ if PA(S_m) > PA($[D\text{-}H]^\bullet$)

30 $M + [S_m + H]^+ \rightarrow [M + H]^+ + S_m$ if PA(M) > PA(S_m)

31 $M^{+\bullet} + S_m \rightarrow [M + H]^+ + [S_m - H]^\bullet$

In negative APPI, the ionizing electrons originate from the dopant (reaction 21), or possibly from the metal surfaces in the ion source [43]. The ionization reactions are similar to those in negative APCI (reactions 12-19), producing $M^{-\bullet}$, $[M-H]^-$, or $[M-X+O]^-$ ions.

Advantages of APPI over ESI are similar to the advantages of APCI, with the addition that, with APPI, completely nonpolar compounds can be ionized. APPI is thus suitable for coupling both LC and GC to MS [44-46].

2.2 Miniaturized spray ionization techniques

Miniaturization of ion sources for MS, including ESI, APCI, and APPI ion sources, has attracted much attention in recent years thanks to the many advantages that miniaturized ion sources provide over conventional systems. Several reviews have been published [1-4]. Most effort has gone into the miniaturization of ESI [47], in the form of nanospray, for example. The flow rates in miniaturized ESI (nL/min) are compatible with those in microfluidic devices. Other miniaturized ion sources – heated nebulizer microchips – have been introduced within just the past few years. The heated nebulizer microchip can be operated in various modes, including APCI (µAPCI) [48], APPI (µAPPI) [49], sonic spray ionization (SSI) [50], thermospray ionization (µAPTSI) [51], and ionspray ionization [52].

The heated nebulizer microchip is a microfabricated device which produces a confined plume (cross-section ~ 1 mm) of sample and solvent vapor mixed with nebulizer/auxiliary gas. The ionization of gas-phase analytes is initiated by corona discharge (in µAPCI) or by photons emitted from a UV lamp (in µAPPI). µAPCI and µAPPI allow the use of lower liquid flow rates (0.05-5 µL/min) than do conventional APCI and APPI (100 µL/min) [48,49], and they are used to couple capillary liquid chromatographs (cap LCs) [53,54] or gas chromatographs (GCs) [54,55] with mass spectrometers with an API source. µAPCI and µAPPI have been shown to provide sensitive and quantitative analysis of steroids [53,54,56] and polycyclic aromatic hydrocarbons [54]. In addition, the heated nebulizer microchip can be used as a heated sprayer in desorption atmospheric pressure photoionization (DAPPI) [8] (see section 2.3).

2.3 Ambient desorption/ionization techniques

Unlike the techniques described in section 2.2, which typically include sample pretreatment and chromatographic separation before ionization, the techniques referred to as “atmospheric pressure surface sampling” [6] or “ambient desorption/ionization” [5] for MS require minimal or even no sample pretreatment, and allow direct sampling of the analyte in ambient conditions. Direct analysis of solid samples, such as tablets or plant parts, then becomes possible. Sampling (desorption) and ionization of analytes are carried out directly from the sample surface outside the mass spectrometer. Following upon the introduction of desorption electrospray ionization (DESI) in 2004 [7] and direct analysis in real time (DART) in 2005 [57], a multitude of ambient desorption/ionization (D/I) techniques have been published [5,6,58,59].

Selected ambient D/I techniques are presented in Table 1. Analyte sampling and ionization can be done simultaneously, as in DESI, or separately, as in desorption atmospheric pressure photoionization (DAPPI) [8]. One of the most popular desorption methods is thermal desorption. Thermal desorption of analytes is carried out by heated gas flow, surface heating, or a combination of these. Other desorption methods include laser beam, neutral droplets or gas impact on a surface, and extraction by liquid stream. The ionization step is typically based on APCI, APPI, or ESI.

Table 1. *Characteristics of selected ambient desorption/ionization techniques. Modified from Van Berkel et al.* [6].

Driving force in surface sampling	Dominant ionization process	Technique name	Acronym	Selected references
Heated gas flow, surface heating, or combination	Liberation of organic salts from surface	Atmospheric pressure thermal desorption / ionization	APTDI	[60]
	APCI - corona discharge	Thermal desorption / atmospheric pressure chemical ionization	TD/APCI	[61]
		Atmospheric pressure solids analysis probe	ASAP	[62]
		Laser diode thermal desorption	LDTD	[63]
		Desorption atmospheric pressure chemical ionization	DAPCI	[64]
	APCI-like	Direct analysis in real time	DART	[57]
		Plasma-assisted desorption / ionization	PADI	[65]
		Dielectric barrier discharge ionization	DBDI	[66]
		Atmospheric pressure glow discharge desorption ionization	APGDDI	[67]
	APPI	Desorption atmospheric pressure photoionization	DAPPI	[8]
Laser beam surface impact	Secondary ionization by ICP	Laser ablation / inductively coupled plasma	LA/ICP	[68,69]
	Secondary ionization by APCI	Laser desorption / atmospheric pressure chemical ionization	LD/APCI	[70]
	Secondary ionization by ESI	Electrospray assisted laser desorption / ionization	ELDI	[71]
		Laser ablation with electrospray ionization	LAESI	[72]
		Infrared laser assisted desorption electrospray ionization	IR LADESI	[73]
Charged droplet / gas jet surface impact	ESI-like	Desorption electrospray ionization	DESI	[7,74]
Neutral droplet / gas jet surface impact	SSI-like	Desorption sonic spray ionization	DeSSI	[75-77]
Gas jet surface impact	Secondary ionization by ESI	Neutral desorption extractive electrospray ionization	NDEESI	[78]
Extraction using a confined liquid stream with liquid microjunction surface contact	ESI	Liquid microjunction surface-sampling probe	LMJ-SSP	[79]
Extraction by confined liquid stream with a sealed surface contact	ESI	Sealing surface-sampling probe	SSSP	[80]

Ambient desorption/ionization techniques used in this work – DESI and DAPPI

In DESI, analytes are picked up from a surface by charged droplets (with diameter of ~ 10 µm or less) (Figure 1). Charged droplets, created by the DESI sprayer, impact the sample surface at high speed (in excess of 100 m/s), form a solvent layer on the sampling surface, and dissolve the analytes [5]. Later-arriving droplets desorb the dissolved analytes, which are subsequently ionized by ESI mechanism (see section 2.1). In general, applications utilizing DESI [81] are restricted to the analysis of relatively polar compounds, although the analysis of neutral and nonpolar compounds (cholesterol and saturated hydrocarbons) has been demonstrated with reactive DESI, which relies on adduct formation [82,83].

Another ambient D/I technique, DAPPI (Figure 2), efficiently desorbs and ionizes neutral and even completely nonpolar analytes [8]. In DAPPI, a heated jet consisting of auxiliary gas and spray solvent vapor desorbs solid analytes from a surface, after which the ionization of analytes takes place in gas phase. The gas-phase ionization mechanism in DAPPI [8] is assumed to be similar to that in APPI (see section 2.1), forming mainly $M^{+\bullet}$ ions (reaction 22, section 2.1) or $[M+H]^+$ ions (reaction 30, section 2.1) depending on the analyte and the spray solvent. With the ability to ionize neutral and nonpolar compounds, DAPPI opens up important new possibilities, for example in the analysis of PAHs, whose analysis is challenging by DESI.

Ambient desorption/ionization applications

Ambient D/I techniques are feasible for analyses where exact quantitation is not needed and fast qualitative screening is sufficient. Fast surface sampling with minimal sample preparation enables high-throughput analysis. In addition, imaging of complex samples, for example tissue sections, is possible since the analytes can be desorbed and ionized directly from the sample surface.

Ambient ionization techniques have been most widely used in pharmaceutical and forensic analysis (Table 2), but also in environmental analysis, such as the analysis of explosives in contaminated groundwater [84] and phytocompouds in plants [7,62,85-88], and in bioanalysis, such as the analysis of lipids in tissues [82,85,89-92].

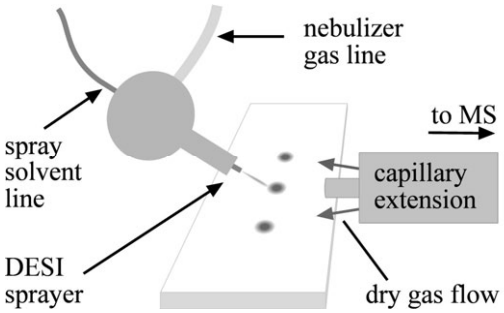

Figure 1 *Schematic view of DESI. Charged droplets generated by the DESI sprayer desorb the analytes from the sampling surface by pick-up mechanism. Analytes are subsequently ionized by ESI mechanism and the analyte ions are introduced to the MS through the capillary extension. The spray solvent line is grounded and the capillary extension of the MS is set at high voltage, for example -4 kV or 4 kV depending on the polarity.*

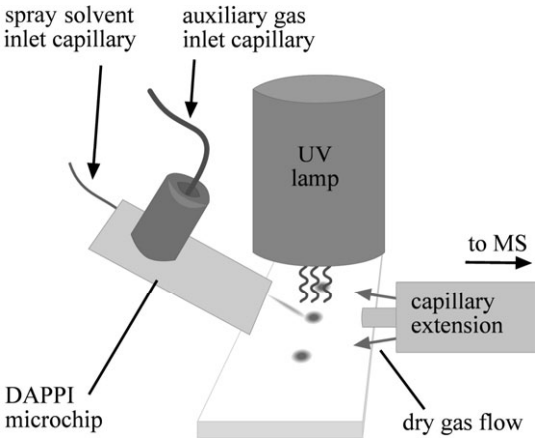

Figure 2 *Schematic view of DAPPI. The heated jet desorbs the analytes from the surface, after which the analytes are ionized in gas phase by photons emitted by the krypton discharge lamp, and the analyte ions are finally introduced to the MS through the capillary extension. The capillary extension of the MS is set at high voltage, for example -4 kV or 4 kV depending on the polarity.*

Table 2. *Examples of analyses of authentic samples carried out by ambient desorption/ionization-mass spectrometry.*

Matrix	Analytes	D/I technique	Ref.
Bioanalysis			
Dog bladder	Glycerophospholipids, sphingolipids, fatty acids	DESI	[89]
Human serum	Cholesterol	reactive DESI	[90]
Mouse brain	Cholesterol	DAPPI	[85]
Mouse brain	Phospholipids, cholesterol	DESI	[85]
Rat brain	Phospholipids, cholesterol	reactive DESI	[90]
Rat brain	Lipids	DESI	[91]
Porcine and rabbit adrenal glands	Catecholamines, lipids	DESI	[82]
Porcine brain extract and rat brain	Phospholipids, sphingolipids	DESI	[92]
Environmental and food analysis			
Coffee bean, tea leaf	Caffeine	APGDDI	[67]
Conium (hemlock) seed and stem	γ-Coniceine	DESI	[7]
Contaminated groundwater	TNT, TNB, RDX, HMX	DESI	[84]
Fruit and vegetable extracts	Carbendazim, imazalil, azoxystrobin, buprofezin, thiabendazole, malathion	DESI	[93]
Grapefruit peel	Imazalil, thiabendazole	DESI	[93]
Hibiscus flower	Essential oils, carotenoids, antioxidants	DESI	[7]
Lemon peel	Thiabendazole	APGDDI	[67]
Lemon peel	Imazalil	DESI	[93]
Salvia (sage) leaf	Tocopherol, carnosol, methyl carnosic acid	DAPPI	[85]
Seaweed	Bromophycolides	DESI	[86,87]
Stevia dietary supplement	Diterpene glycosides, fructose oligomers	DESI	[88]
Spinach leaf	Carotenoids	DART	[62]
Tomato skin	Lycopene and other carotenoids	DESI	[7]
Pharmaceutical and forensic analysis			
Bank note	Cocaine, aspirin	DART	[62]
Cannabis flower and resin	Δ-9-THC, cannabinol	DAPPI	[94]
Cannabis leaf	Δ-9-THC, cannabinol	DESI	[95]
Confiscated blotter paper	LSD, ABDF	DAPPI	[94]
Confiscated drug tablets	MDMA, amphetamine, phenazepam, buprenorphine	DAPPI	[94]
Ecstasy tablets	MDMA, methamphetamine, amphetamine, caffeine, MBDB, 4-MTA	DESI	[96]
Human skin surface	Loratadine	DESI	[7]
Ibuprofen tablet	Ibuprofen	APGDDI	[67]
Mouse whole body tissue section	Propranolol	DESI	[97]
Rat brain, lung, kidney, and testis	Clozapine, N-desmethyl metabolite (only in lung)	DESI	[98]
Tenox tablet	Temazepam	DAPPI	[8]
Tylenol tablet	Paracetamol	APGDDI	[67]
Tylenol tablet	Paracetamol, pseudoephedrine, dextromethorphane, chlorpheniramine	DAPPI	[8]
Urine	Amphetamines, opiates, cannabinoids, benzodiazepines	DESI	[99]
Other			
Perfumes	Fingerprints of authentic and counterfeit perfumes	EASI	[100]

Abbreviations for analytes in Table 2:

ABDF	Bromobenzodifuranylisopropylamine, Bromo-DragonFLY
HMX	Octahydro-1,3,5,7-tetranitro-s-tetrazocine
LSD	Lysergic acid diethylamide
MBDB	*N*-Methyl-1-(1,3-benzodioxol-5-yl)-2-butanamide
MDMA	3,4-Methylenedioxymethamphetamine, Ecstasy
4-MTA	4-Methylthioamphetamine
Δ-9-THC	Δ-9-Tetrahydrocannabinol
RDX	1,3,5-Trinitro-1,3,5-triazacyclohexane
TNB	1,3,5-Trinitrobenzene
TNT	2,4,6-Trinitrotoluene

3 Analysis of environmental samples and biosamples

Chemical analyses of environmental samples and biosamples are required to estimate the risks that compounds pose to humans and animals, to support decision-making about legislation and protection, and to monitor and control the use of licit and illicit drugs. The most extensively used analytical techniques for environmental analysis [18] and bioanalysis [101,102] are GC-MS and LC-MS. The literature review in this chapter concentrates on the mass spectrometric analysis methods of the compounds studied in this thesis.

MS is a versatile technique because it offers information not only about the molecular mass but also the molecular structure of the analyte. Compounds are identified on the basis of accurate masses of their ions, which means that even complex mixtures of compounds can be analyzed, particularly in the case of an MS instrument with high resolving power [103]. Since the sample matrix disturbs the analysis, samples typically need to be prepared before analysis. Sample pretreatment, indeed, remains the bottleneck in the whole analytical process, and developments allowing fast pretreatment, or even the absence of pretreatment, will contribute most to speeding up the process.

The miniature ionization techniques for MS, introduced in Chapter 2, offer advantages over the techniques used in conventional MS systems. µAPCI and µAPPI enable the coupling of micro liquid separation systems or GC with MS. Further, they allow very low sample solution flow rates (0.05–5 µL/min) [48,49], which make them suitable for analytical applications where sample volumes are limited. In the case of GC, µAPCI and µAPPI enable coupling of a GC with MS instruments with API interface, instruments that are usually used only with LC. In addition, the use of µAPCI and µAPPI offers more intense molecular ion peaks in mass spectra than can be achieved with conventional GC-EI-MS instruments. Ambient D/I techniques, such as DAPPI, offer fast and direct analysis of analytes on surfaces without sample pretreatment.

The conventional MS methods used to analyze the compounds investigated in this study are reviewed below.

Mass spectrometric analysis of PCBs, PAHs, BFRs, and pesticides

The environmental pollutants studied in this work included PCBs (congener Nos. 28, 52, 101, 118, 138, 153, and 180) (**I**), PAHs (anthracene, benzo[a]pyrene (BaP), benzo[k]fluoranthene (BkF), chrysene, naphthalene, and phenanthrene) (**IV**), one brominated flame retardant (BFR) (tetrabromobisphenol A (TBBPA)) (**IV**), and pesticides (aldicarb, carbofuran, ditalimfos, imazalil, methiocarb, methomyl, oxamyl, pirimicarb, and thiabendazole) (**IV**). Structures of the analytes are presented in Figure 3 (section 5.1). The conventional chromatographic and mass spectrometric methods for investigating these compounds are noted below.

GC is usually the method of choice for chromatographic separation of thermally stable and volatile environmental analytes such as PCBs [104], PAHs [105], BFRs [106], and pesticides [107]. Analytes eluting from a GC are ionized by electron ionization (EI) or chemical ionization (CI), depending on the nature of the analytes and the application. LC coupled with MS is preferred for more polar, thermally unstable, non-volatile or high-molecular-mass compounds, such as PAHs with high boiling point or nitrated PAHs [108], certain BFRs (e.g., TBBPA) [109], and certain pesticides [110,111]. Ionization

methods for LC-MS include ESI, APCI, and APPI. Environmental samples are almost always pretreated before analysis, for example by sieving, grinding, and extraction [112]. Typical sample matrices in environmental analysis include soil [113,114], sediment [108,115], sewage sludge [116], indoor dust [117], natural and treated water [108,110,115], air [115,117,118], and food [111,115,119,120].

Mass spectrometric analysis of SARMs and drugs

Bioanalytical applications descibed in this thesis include the analysis of 2-quinolinone-derived SARMs (6-*N*,*N*-bis(2,2,2-trifluoroethyl)amino-4-trifluoromethylquinolin-2(*1H*)-one (SARM A), 6-*N*,*N*-bisethylamino-4-trifluoromethylquinolin-2(*1H*)-one (SARM B), 6-*N*-propylamino-4-trifluoro-methylquinolin-2(*1H*)-one (SARM C)) (**II**), and the analysis of illicit drugs (amphetamine, cocaine, heroin, methamphetamine, 3,4-methylenedioxymethamphetamine (MDMA)) (**V**). Structures of the compounds are presented in Figure 3 (section 5.1). The conventional chromatographic and mass spectrometric methods for analysis of these compounds are noted below.

SARMs are a diverse class of compounds with anabolic activity similar to that of anabolic steroids but without androgenic activity. Thus, SARMs are attractive not only in the treatment of diseases but also as dopants in sports. Screening for SARMs in doping testing is becoming of increasing importance in pace with the growing abuse of SARM compounds [16]. Reported analytical methods for the novel 2-quinolinone-derived SARMs include LC-ESI-MS [121] and GC-EI-MS [122]. Mass spectrometric analysis of other SARM groups has been reviewed elsewhere [123].

Chemical analyses of drug compounds in various forms and matrices, such as tablets and powders [124-126], traces on surfaces [127], biological fluids (urine [128] and blood [129]), hair [130,131], or plants [132-134] are important in chemical finger-printing of illicit drugs, control of illegal use of drugs, and clinical and forensic toxicology. Volatile and semivolatile compounds are usually investigated by GC-MS and nonvolatile and thermolabile compounds by LC-MS. Extensive sample preparation is often required for biological sample matrices [135], while minimal preparation is usually enough for tablets and powders. In addition to GC-MS and LC-MS techniques, ambient desorption/ionization-MS has been exploited in the analysis of samples for illicit drugs since it offers the possibility for fast screening without sample preparation. DESI-MS and DAPPI-MS applications reported for drug analysis include the analysis of ecstasy tablets [94-96], blotter paper [94], *Cannabis sativa* plant (leaf [95], flower and resin [94]), and various drugs in urine [99].

4 Aims of the study

The overall aim of the study was to demonstrate the feasibility of novel miniaturized API techniques for MS for environmental analysis and bioanalysis. The ionization techniques investigated were µAPCI, µAPPI, and DAPPI. The first two techniques can be coupled with chromatographic separation (GC-µAPCI-MS and GC-µAPPI-MS) (**I**, **II**), whereas the latter (DAPPI-MS) can be utilized in direct ambient sampling without a separation stage or other sample pretreatment (**III**, **IV**, **V**). For comparison, DESI-MS analysis was performed alongside DAPPI-MS analysis (**V**).

In more detail the aims of the study were

- to couple GC to MS with an API microchip (GC-µAPCI-MS and GC-µAPPI-MS) (**I**, **II**)
- to evaluate the analytical characteristics of µAPCI and µAPPI (**I**)
- to show the feasibility of GC-µAPCI-MS and GC-µAPPI-MS in environmental analysis (**I**) and bioanalysis (**II**)
- to study the desorption and ionization mechanisms in DAPPI (**III**)
- to develop rapid DAPPI-MS screening methods for analytes with various physicochemical properties (**IV**, **V**)
- to show the suitability of DAPPI-MS methods in real-life analytical work (**IV**, **V**)

5 Experimental

This chapter briefly described the chemicals, samples, and instrumentation used in the work. More detailed descriptions can be found in the original Papers **I–V**.

5.1 Chemicals and materials

Table 3 lists the products and materials used in the work, Table 4 the samples, and Table 5 the chemicals. The structures of the studied compounds are presented in Figure 3.

Table 3. *List of products and materials.*

Product / Material	Manufacturer / Supplier	Paper
Aluminum plate, thickness 3 mm	Tibnor Ltd., Espoo, Finland	III
Aluminum foil, thickness 15 µm	Metsä Tissue, Mänttä, Finland	III
BPX5 analytical GC column	SGE Analytical Science Pty Ltd., Ringwood, Australia	II
Copy/print paper	UPM Kymmene, Kuusankoski, Finland	III
Deactivated silica capillary, 150 µm i.d., 220 µm o.d.	SGE Analytical Science Pty Ltd., Ringwood, Australia	I, II
Deactivated silica capillary, 50 µm i.d., 220 µm o.d.	SGE Analytical Science Pty Ltd., Ringwood, Australia	III, IV, V
Double-sided tape	Scotch, Cergy-Pontoise, France	III, IV
Duralco 4703, high-temperature resistant epoxy glue	Cotronics Corp., Brooklyn, NY, USA	I, II, III, IV, V
Filter paper	Schleicher & Schuell GmbH, Dassel, Germany	III
Kitchen paper	Metsä Tissue, Mänttä, Finland	III
Microscope glass slide	Menzel GmbH + Co KG, Braunschweig, Germany	III
Nanoport fluidic connector	Upchurch Scientific Inc. Oak Harbor, WA, USA	I, II, III
Oasis HLB SPE cartridges, 3 cc	Waters, Milford, MA, USA	II
Poly(methyl methacrylate) (PMMA)	Vink Finland Ltd., Kerava, Finland	III, IV, V
Poly(tetrafluoroethylene) (PTFE)	Vink Finland Ltd., Kerava, Finland	III
Silicon plate, thickness 0.5 mm	Okmetic, Vantaa, Finland	III
Tecasint 2011 amorphous polyimide	Ensinger GmbH, Nutfringen, Germany	IV
Thin-layer chromatography plate	Merck KGaA, Darmstadt, Germany	III
Tylenol Cold tablets	McNeil PPC Inc., Fort Washington, PA, USA	III
VF 5-ms analytical GC column	Varian Inc., Middelburg, The Netherlands	I

Table 4. *Samples.*

Sample	Origin	Paper
Circuit board	Workshop at the University of Helsinki, Finland	IV
Confiscated drug powders	National Bureau of Investigation, Vantaa, Finland	V
Contaminated soil	Helsinki district, Finland	I
Oranges	Grocery store, Helsinki, Finland	IV
Humic soil	Eno, Finland	IV

Table 5. *List of chemicals used in the experiments.*

Chemical	Manufacturer / Supplier	Paper
Acetic acid	Mallinckrodt Baker B.V., Deventer, The Netherlands	II
Acetic acid	VWR International, Briane, France	IV
Acetone	Mallinckrodt Baker B.V., Deventer, The Netherlands	III, V
Acetone	Labscan Ltd., Dublin, Ireland	IV
Acridine	Sigma-Aldrich, Steinheim, Germany	IV
Aldicarb	Sigma-Aldrich, Steinheim, Germany	IV
Anisole	Fluka Chemie GmbH, Buchs, Switzerland	III, IV
Anthracene	Sigma-Aldrich, Steinheim, Germany	III
Benzo[a]pyrene	Sigma-Aldrich, Steinheim, Germany	III, IV
Benzo[k]fluoranthene	Sigma-Aldrich, Steinheim, Germany	IV
6-*N*,*N*-Bis(2,2,2-trifluoroethyl)amino-4-trifluoromethylquinolin-2(*1H*)-one	Institute of Biochemistry, German Sports University, Cologne, Germany	II
6-*N*,*N*-Bisethylamino-4-trifluoromethylquinolin-2(*1H*)-one	Institute of Biochemistry, German Sports University, Cologne, Germany	II
Carbofuran	Sigma-Aldrich, Steinheim, Germany	IV
Chloroform	VWR International, Leuven, Belgium	I
Chrysene	Sigma-Aldrich, Steinheim, Germany	IV
Dichloromethane	Merck, Darmstadt, Germany	I
1,4-Dinitrobenzene	Sigma-Aldrich, Steinheim, Germany	III
Ditalimfos	Sigma-Aldrich, Steinheim, Germany	IV
Ethyl acetate	Sigma-Aldrich, Buchs, Switzerland	II
Formic acid	Acros Organics, Geel, Belgium	V
β-Glucuronidase, type HP-2	Sigma-Aldrich, Buchs, Switzerland	II
Helium 99.996%	AGA, Espoo, Finland	I, II
Heptane	Lab-Scan, Dublin, Ireland	I
Hexachlorobenzene	Sigma-Aldrich, Steinheim, Germany	I
Hexane	Lab-Scan, Dublin, Ireland	I
Hexane	Mallinckrodt Baker B.V., Deventer, The Netherlands	III
Imazalil	Sigma-Aldrich, Steinheim, Germany	IV
Isopropanol	Lab-Scan, Dublin Ireland	III
Methanol	Mallinckrodt Baker B.V., Deventer, The Netherlands	II, III, V
Methanol	Labscan Ltd., Dublin, Ireland	IV
Methiocarb	Sigma-Aldrich, Steinheim, Germany	IV
Methomyl	Sigma-Aldrich, Steinheim, Germany	IV
3,4-Methylenedioxymethamphetamine	United Laboratories Ltd., Helsinki, Finland	III
Naphthalene	Fluka Chemie, Buchs, Switzerland	IV
Naphthoquinone	Sigma-Aldrich, Steinheim, Germany	III
Naphthoic acid	Sigma-Aldrich, Steinheim, Germany	III
Nitrogen, from liquid nitrogen	AGA, Espoo, Finland	III, IV, V
N-Methyl-*N*-(trimethylsilyl)trifluoroacetamide	Sigma-Aldrich, Buchs, Switzerland	II
6-*N*-Propylamino-4-trifluoromethylquinolin-2(*1H*)-one	Institute of Biochemistry, German Sports University, Cologne, Germany	II
Oxamyl	Sigma-Aldrich, Steinheim, Germany	IV
Paracetamol	Merck, Darmstadt, Germany	III
Polychlorinated biphenyls, Nos. 28, 52, 101, 118, 138, 153, 180	Nab Labs Inc., Helsinki, Finland	I
Phenanthrene	Sigma-Aldrich, Steinheim, Germany	IV
Pirimicarb	Sigma-Aldrich, Steinheim, Germany	IV
Sodium acetate	Sigma-Aldrich, Buchs, Switzerland	II
Sulfuric acid	Merck, Darmstadt, Germany	I
Testosterone	Fluka Chemie GmbH, Buchs, Switzerland	III
Tetrabromobisphenol A	Sigma-Aldrich, Steinheim, Germany	IV
Tetracyclone	Sigma-Aldrich, Steinheim, Germany	III
Thiabendazole	Sigma-Aldrich, Steinheim, Germany	IV
Toluene	Mallinckrodt Baker B. V., Deventer, The Netherlands	I
Toluene	Sigma-Aldrich, Buchs, Switzerland / Steinheim, Germany	II, IV
Toluene	Lab-Scan Ltd., Dublin, Ireland	III, V
Verapamil hydrochloride	Sigma-Aldrich, Steinheim, Germany	III

Paper I

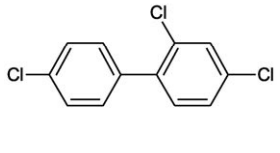

PCB 28 (255.96)

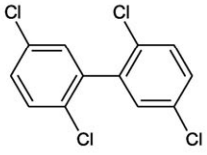

PCB 52 (289.92)

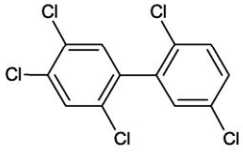

PCB 101 (323.88)

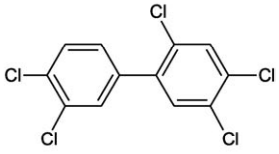

PCB 118 (323.88)

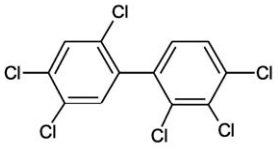

PCB 138 (357.84)

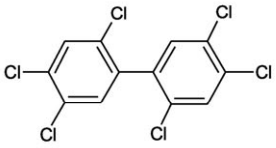

PCB 153 (357.84)

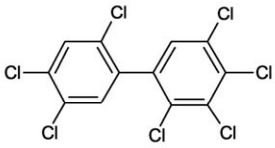

PCB 180 (391.81)

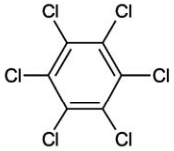

Hexachlorobenzene (HCB) (281.81)

Paper II

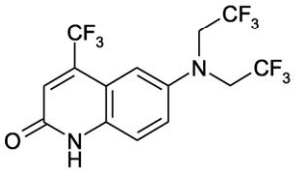

6-*N*,*N*-Bis(2,2,2-trifluoroethyl)amino-4-trifluoromethylquinolin-2(*1H*)-one (SARM A) (392.06)

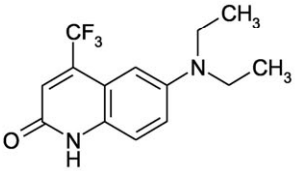

6-*N*,*N*-Bisethylamino-4-trifluoromethylquinolin-2(*1H*)-one (SARM B) (284.11)

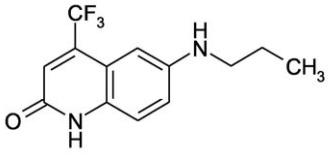

6-*N*-Propylamino-4-trifluoro-methylquinolin-2(*1H*)-one (SARM C) (270.10)

Paper III

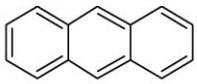

Anthracene (178.08)

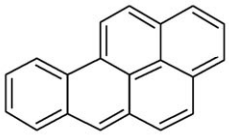

Benzo[a]pyrene (BaP) (252.09)

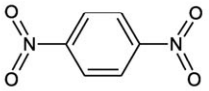

1,4-Dinitrobenzene (168.02)

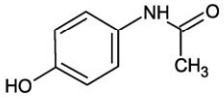

Paracetamol (151.06)

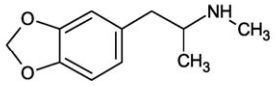

3,4-Methylenedioxymethamphetamine (MDMA) (193.11)

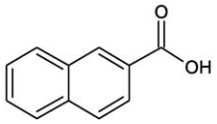

2-Naphthoic acid (172.05)

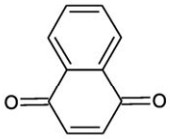

1,4-Naphthoquinone (158.04)

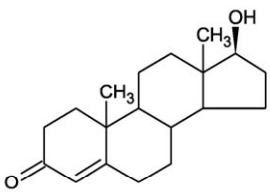

Testosterone (288.21)

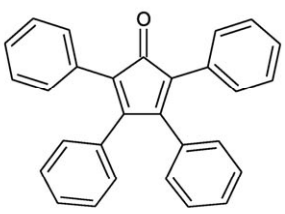

Tetracyclone (384.15)

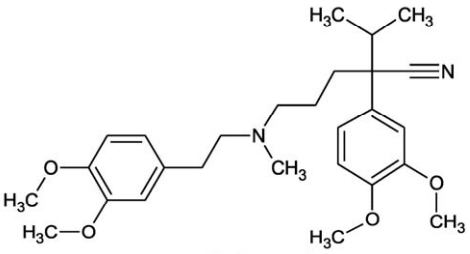

Verapamil (454.28)

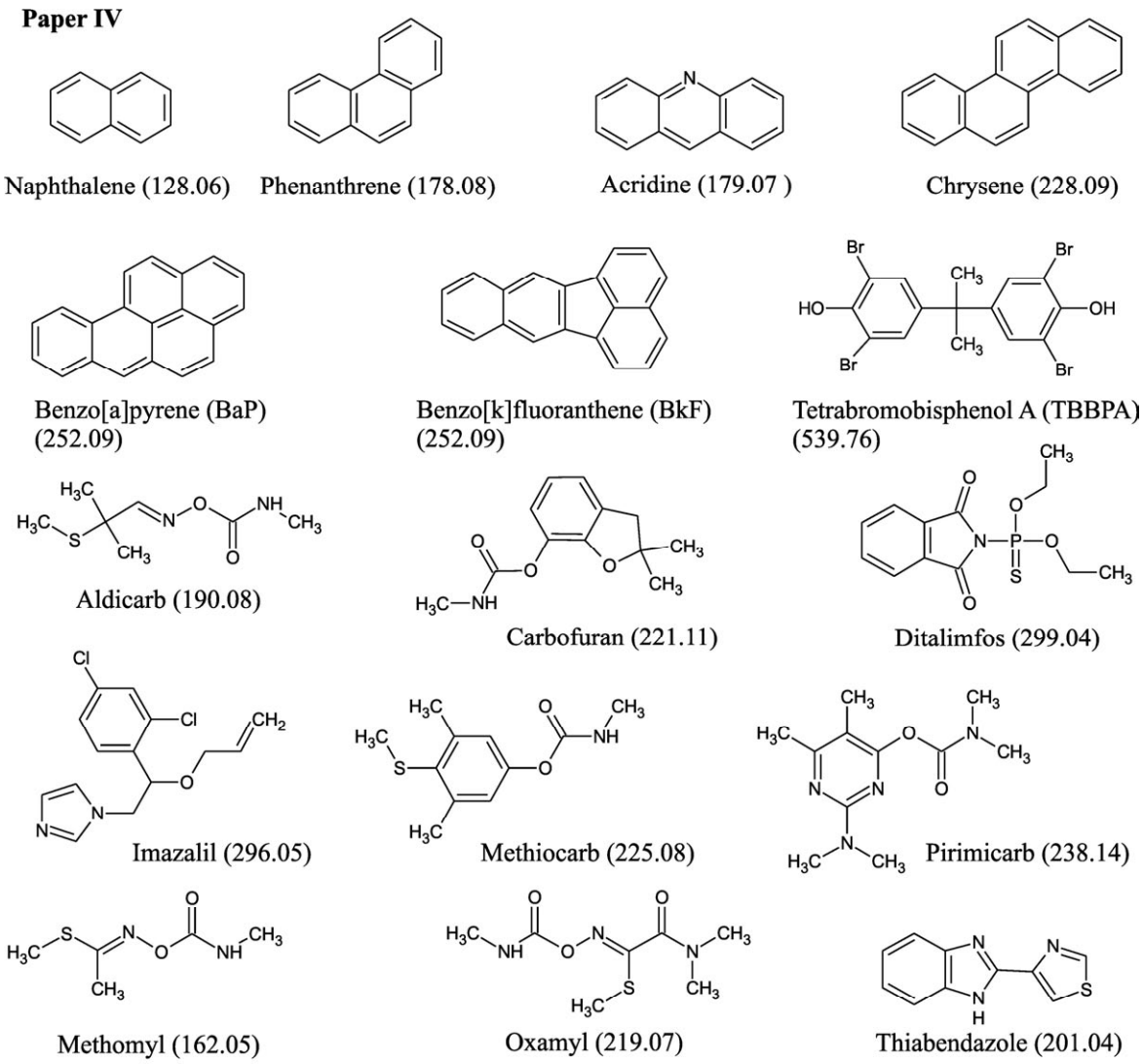

Figure 3 *Structures and monoisotopic masses (g/mol) of compounds investigated in studies **I-V**.*

5.2 Instrumentation

Commercially available instruments are listed in Table 6. The API microchips and the ion sources utilizing them are described in the text below.

Table 6. *Instruments used in the study.*

Instrument	Manufacturer	Publication
Accelerated solvent extractor	Dionex, Sunnyvale, CA, USA	I
API3000 triple quadrupole MS	Applied Biosystems/MDS Technologies, Concord, Canada	II
APPI power source	Elctronics Facility, University of Groningen, The Netherlands	I
Esquire 3000+ ion trap MS	Bruker Daltonics, Bremen, Germany	I, III, IV, V
Capillary extension for Esquire 3000+	Agilent Technologies, Santa Clara, CA, USA	III, IV, V
CTC-A200S autosampler for GC	CTC Analytics, Zwingen, Switzerland	II
Flow Tracker 1000 flow meter	Agilent, Santa Clara, CA, USA	I
GC/FID (HP 6890)	Agilent Technologies, Waldbronn, Germany	V
GC/MS (HP 6890/HP 5973)	Agilent Technologies, Waldbronn, Germany	V
HP 5890 II gas chromatograph	Hewlett-Packard, Waldbronn, Germany	I, II
Hydraulische Presse laboratory press	PerkinElmer, Wiesbaden, Germany	IV
LC/UV (HP 1100)	Agilent Technologies, Santa Clara, CA, USA	V
LTQ Orbitrap	Thermo Fischer Scientific, Bremen, Germany	II
Nanospray stand	Proxeon Biosystems A/S, Odense, Denmark	I, II, III, IV, V
Nitrogen generator	Whatman Inc. Haverhill, MA, USA	II
Nitrogen generator	CMC Instruments, Eschborn, Germany	II
Polymill KCH-Analytical mill A 10	Kinematica AG, Littau-Lucerne, Switzerland	IV
Rotating stage	Newport Corp., Irvine, CA, USA	IV
UV lamp	Cathodeon / Heraeus Noblelight, Cambridge, UK	I, II, III, IV, V
Water purifying system	Millipore, Molsheim, France	II, III, IV, V
Xyz stages	Proxeon Biosystems A/S, Odense, Denmark	III, IV

API microchips and ion sources

In previous papers, the microchips used in µAPCI, µAPPI, and DAPPI were called "heated nebulizer microchips" (see, e.g., [8,48,49,53,54,136]). In the present work with GC-µAPCI-MS and GC-µAPPI-MS (**I**, **II**), however, the sample is in gaseous form and nebulization does not occur. "Heated nebulizer microchip" is regarded as misleading therefore. Although the DAPPI microchip does work as a heated nebulizer microchip, for simplicity's sake the microchips for µAPCI, µAPPI, and DAPPI are all referred to as "API microchips" rather than heated nebulizer microchips.

The API microchip for GC-µAPI-MS applications consisted of silicon and Pyrex glass wafers bonded together by anodic bonding [48] (Figure 4a and Figure 4b), whereas the API microchip for DAPPI-MS applications consisted of two Pyrex glass plates bonded together by fusion bonding [137] (Figure 4c and Figure 4d). The microchips included an insertion channel for the sample capillary (GC-µAPI-MS) or the spray solvent capillary (DAPPI-MS), an inlet for the auxiliary gas, a heated mixing channel, and an exit nozzle. The height of the heated mixing channel was 250 µm and the width 800 µm. Detailed fabrication processes for the microchips have been presented elsewhere [48,137]. Deactivated silica capillary (150 µm i.d., 220µm o.d. for GC-µAPI-MS, and 50 µm i.d., 220 µm o.d. for DAPPI-MS) for introduction of the sample (GC-µAPI-MS) or the spray solvent (DAPPI-MS) was attached to the microchip with high temperature-resistant epoxy glue. A Nanoport fluidic connector for the auxiliary gas line connection was either glued with the epoxy glue (**I**), attached with an adhesive pad (**III**, **V**) or pressed tightly against the microchip surface with a custom-made clamp (**II**, **IV**). Wires for the heating power

connection were either soldered on to the platinum heating resistor (**I**, **II**, **III**, **V**) or connected to the resistor with a custom-made clamp (**IV**).

The ion sources utilizing the API microchips – µAPCI, µAPPI, and DAPPI ion sources – are shown in Figure 5a, Figure 5b, and Figure 6, respectively.

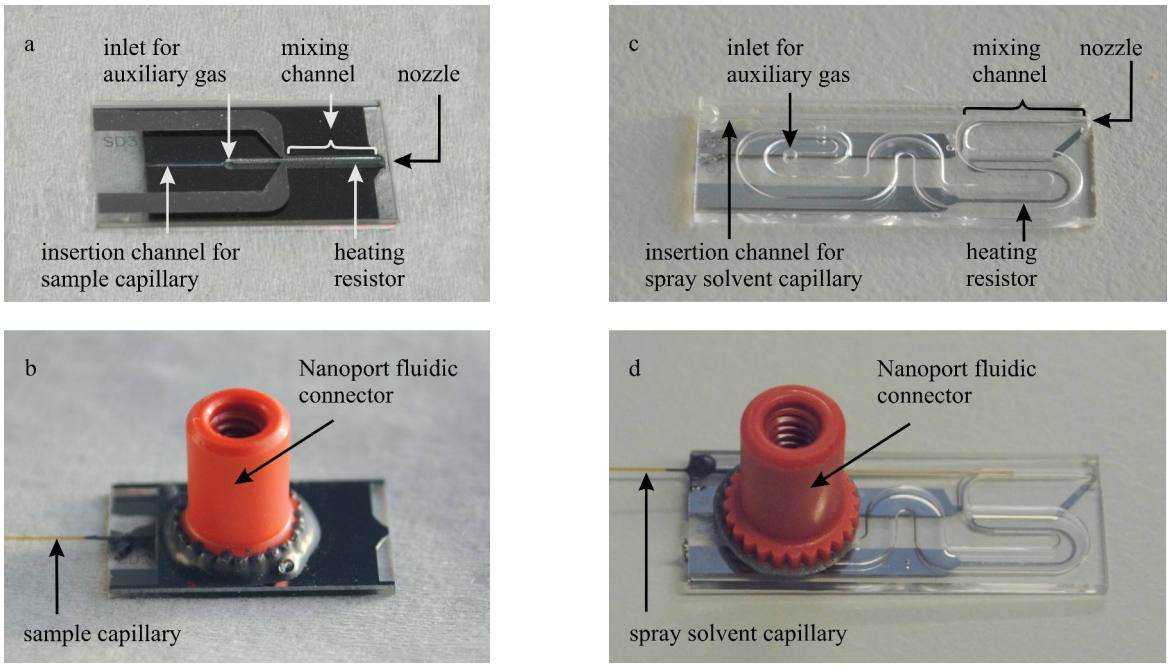

Figure 4 *(a) The API microchip for GC-µAPCI-MS or GC-µAPPI-MS. The microchip measures 18 mm x 10 mm. Panel (b) shows the same microchip as in (a) with a Nanoport fluidic connector and sample capillary. (c) The API microchip for DAPPI-MS. The microchip measures 25 mm x 10 mm. Panel (d) shows the same microchip as in (c) with a Nanoport fluidic connector and spray solvent capillary.*

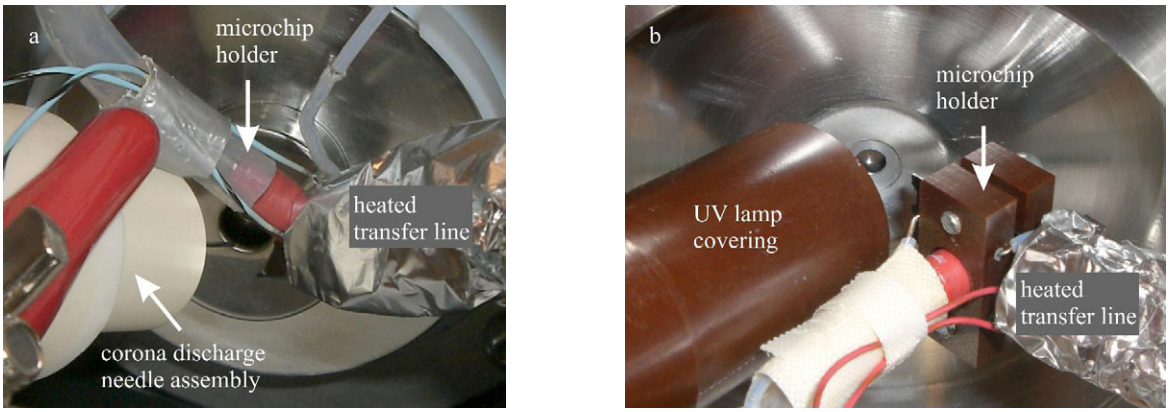

Figure 5 *(a) Ion source configuration for GC-µAPCI-MS. Heated transfer line between the GC and the µAPCI is seen on the right, microchip in the middle, heating power wires and microchip holder with integrated auxiliary gas line in the upper left quarter, and the corona discharge needle assembly in the lower left quarter. The µAPCI ion source is placed in front of the spray shield of the Esquire 3000+ ion trap MS. (b) Ion source configuration for GC-µAPPI-MS. Heated transfer line between the GC and the µAPPI is seen in the lower right corner, holder for the µAPPI including connections for auxiliary gas and for heating power wires in the middle, and the covering of the krypton discharge lamp on the left. The µAPPI ion source is placed in front of the orifice of the API3000 triple quadrupole MS.*

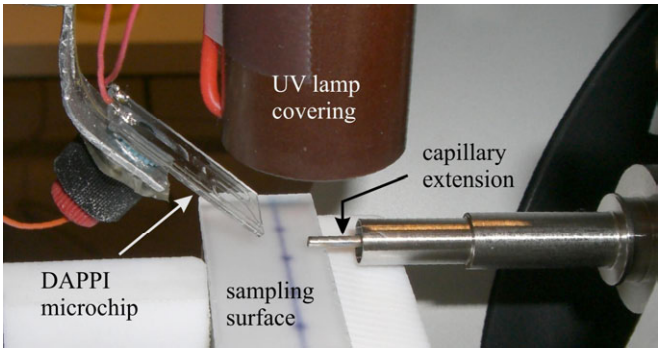

Figure 6 *Setup of the DAPPI ion source. The DAPPI microchip, made of glass, is seen on the left, covering of the UV lamp on top, the capillary extension of the MS capillary on the right, and the polymer sampling surface in the middle. A schematic view of the DAPPI ion source is presented in Figure 2.*

6 Results and discussion

6.1 GC-µAPI-MS

This section summarizes the results presented in Papers **I** and **II**. The first goal of the experiments was to show that µAPCI and µAPPI can be applied in the coupling of commercial instruments. A GC was coupled with an ion-trap MS (**I**), a triple quadrupole MS (**II**), and an Orbitrap MS (**II**), after which analytical applications were carried out with the instrumentation. Paper **I** presents the analysis of PCBs by GC-µAPCI-MS and GC-µAPPI-MS methods in negative ion mode. Analytical characteristics (e.g., limits of detection (LODs)) of the methods were studied by analyzing standard compounds, after which the feasibility of the method for real-life analytical work was demonstrated by analysis of PCBs in contaminated soil. The quantitation results from soil extracts obtained by GC-µAPPI-MS method were then compared with the results obtained by conventional GC-ECD method. Paper **II** presents the analysis of SARMs by GC-µAPPI-triple quadrupole MS and GC-µAPCI-Orbitrap MS methods in positive ion mode. Analytical characteristics of the GC-µAPPI-triple quadrupole MS method were determined with spiked urine. The proof-of-concept of the GC-µAPCI-Orbitrap MS technique was demonstrated in an analysis of standard compounds.

6.1.1 Chromatography

The GC conditions were optimized for fast and efficient separation. Full-scan chromatograms and mass spectra were recorded to determine the retention times of the analytes.

Extracted ion chromatograms of seven PCB congeners (Nos. 28, 52, 101, 118, 138, 153, and 180) (**I**) and three SARMs (SARM A, B, and C) (**II**) are presented in Figure 7 and Figure 8, respectively. The GC-µAPCI-MS and GC-µAPPI-MS analyses of the PCBs were performed in full-scan MS mode with an ion trap MS at mass range m/z 220–400, since PCBs did not produce any detectable product ions in MS/MS fragmentation experiments. The width of the *m/z* window for the EICs in Figure 7 is approx. 10 *m/z* units for each analyte. The marked differences in the mass spectrometric responses of the various PCB congeners were attributed to their diverse EAs. For example, calculated EAs for PCB 52 and PCB 118 are 0.61-0.69 eV and 0.91-0.95 eV, respectively [138].

Based on MS/MS fragmentation experiments with SARMs (see discussion in section 6.1.2), GC-µAPPI-MS/MS analysis of SARMs was performed in SRM mode from $M^{+\bullet}$ ions with three SRM ion pairs per compound (Table 9, section 6.1.4). Figure 8a shows the SRM chromatograms of the analytes in urine obtained by summing all the SRM ion pairs, while Figure 8b shows the SRM chromatograms of the blank urine sample.

Narrow chromatographic peaks in Figure 7 (half-widths ~3 s) and Figure 8a (half-widths 1.2 s) indicate proper functioning of the chromatography and a minimal dead volume in the microchip. The same was demonstrated previously [54,55].

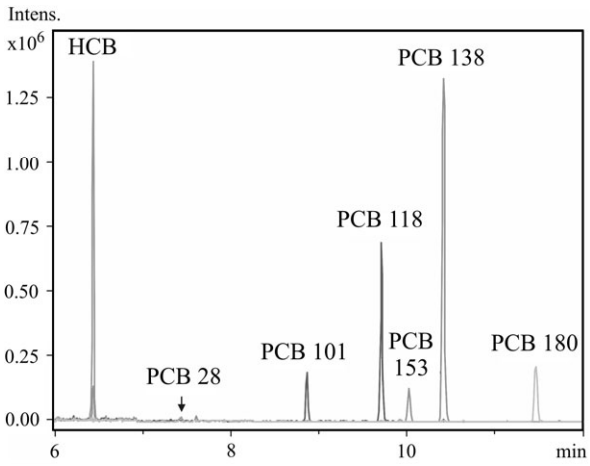

Figure 7 *Extracted ion chromatograms (EICs) of the $[M\text{-}Cl+O]^-$ ions of the PCBs and hexachlorobenzene (HCB, ISTD) from a full-scan run (m/z 220–400) with GC-µAPPI-MS. The width of the EIC window for each analyte is approx. 10 m/z units. The concentration of each analyte was 500 ng/mL and injection (splitless mode) volume was 1 µL.*

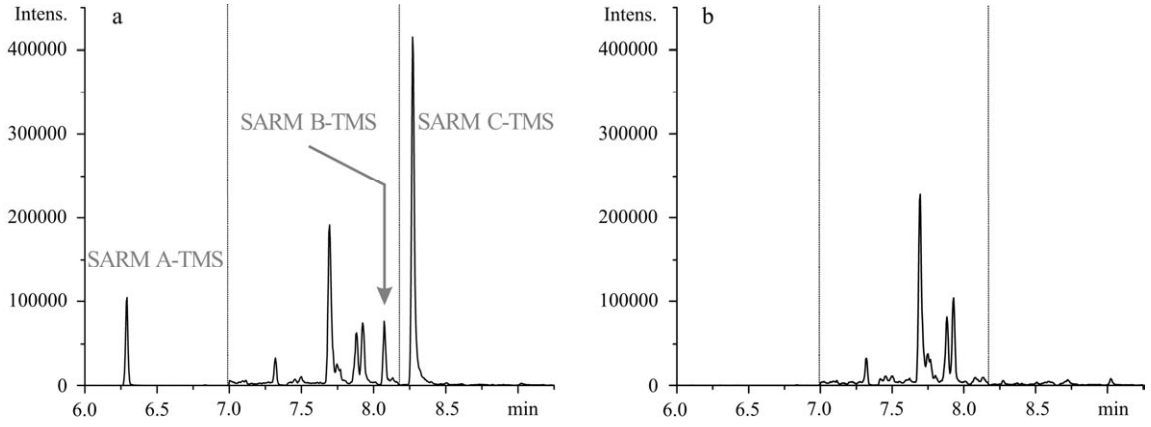

Figure 8 *(a) Selected reaction monitoring (SRM) chromatograms of SARMs (SARMs A, B, and C) with three ion pairs from $M^{+\bullet}$ ions of trimethylsilylated compounds. The analyte concentration was 10 ng/mL of non-derivatized SARMs in urine. (b) SRM chromatograms of a blank urine sample. Injection (splitless mode) volume was 1 µL.*

6.1.2 Ionization and mass spectra

The research presented in Papers **I** and **II** was done with both APCI and APPI, which are related ionization methods in that they often produce the same kind of ions. The ionization reactions taking place in APCI and APPI are presented in section 2.1. Unlike most cases described in the literature, with GC-µAPCI-MS and GC-µAPPI-MS there is no LC solvent present in the ionization area. Thus the reactant ions are formed only from atmospheric gases (nitrogen, oxygen, and water vapor) or from dopant vapor.

PCBs in negative ion mode (I)

Ionization of the PCBs was first studied in infusion experiments with µAPCI-MS and µAPPI-MS. PCBs produced $[M\text{-}Cl+O]^-$ ions in negative ion mode with APCI and APPI with typical chlorine isotopic patterns. Some $M^{-\bullet}$ ions were observed too (Figure 9), but since the signal intensities of the $M^{-\bullet}$ ions were much lower than those of the $[M\text{-}Cl+O]^-$ ions, they were regarded as insignificant. According to Dzidic *et al.* [32], even a trace concentration of oxygen in a nitrogen atmosphere is sufficient for phenoxide ion formation, and thus phenoxide ion formation is expected in open systems, such as µAPCI and µAPPI, even though pure nitrogen is used as auxiliary gas in the API microchip and as dry gas in the MS. The ionization mechanisms were presumably similar to those proposed in section 2.1 (reactions 16 and 17).

Since the $[M\text{-}Cl+O]^-$ ions did not produce detectable MS/MS product ions, the $[M\text{-}Cl+O]^-$ ions were monitored in full-scan MS mode at mass range *m/z* 220–400 in the infusion studies, and also later in the studies with GC (GC-µAPCI-MS and GC-µAPPI-MS). Examples of mass spectra obtained with µAPPI-MS are shown in Figure 9. The spectra show similar isotopic distributions to the theoretically calculated spectra of $[M\text{-}Cl+O]^-$ ions (generated by Bruker Daltonics IsotopePattern software).

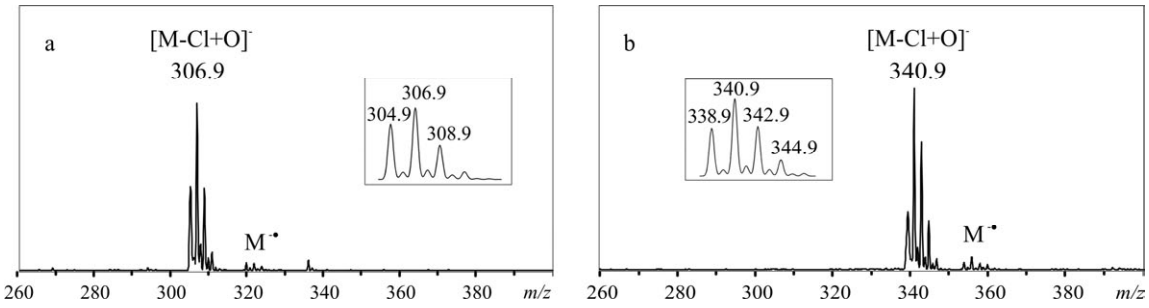

Figure 9 *Full-scan mass spectra of (a) PCB 118 and (b) PCB 138. The chlorine isotopic patterns of the $[M\text{-}Cl+O]^-$ ions show similar distributions to the theoretically calculated spectra (shown as inserts). Other studied congeners and hexachlorobenzene (ISTD) produced similar chlorine isotopic patterns.*

SARMs in positive ion mode (II)

Both APCI and APPI were tested as ionization methods for trimethylsilylated SARMs. APPI produced both radical cations ($M^{+\bullet}$) and protonated molecules ($[M+H]^+$), whereas APCI produced only protonated molecules. The mass spectrometric responses for ionized analytes were at about the same level with the two methods. No fragmentation of analytes was observed in the MS spectra. The ratio of $M^{+\bullet}$ to $[M+H]^+$ signal intensity in APPI was approximately 3:2. The $M^{+\bullet}$ ions in APPI are produced by charge exchange between the ionized dopant (toluene) and analyte molecules (reaction 22, section 2.1), whereas the $[M+H]^+$ ions in both APCI and APPI are produced in the proton transfer reactions between protonated species and the analytes (reactions 6 and 24, section 2.1).

Product ions of both $M^{+\bullet}$ and $[M+H]^+$ precursor ions were studied by infusion experiments with µAPPI-MS/MS. On the basis of these experiments, GC-µAPPI-MS/MS analysis was performed in SRM mode with $M^{+\bullet}$ and $[M+H]^+$ ions as precursor ions, in both cases with three SRM ion pairs (Table 9). The ion pairs from $M^{+\bullet}$ ions showed better signal-to-noise ratios (S/N) than those obtained for the ion pairs from $[M+H]^+$ ions, and thus APPI was selected as the ionization method and $M^{+\bullet}$ ions as the precursor ions. Figure 10 shows the APPI-MS/MS spectra of trimethylsilyl derivatives of SARM A, B, and C. The spectra are the averages of multiple MS/MS spectra obtained with different collision energies in the range 20–65 eV. Some of the mass peaks are easily recognized from the product ion spectra (Figure 10). All the MS/MS spectra show TMS product ions at *m/z* 73; peaks originating from methyl radical losses at *m/z* 449 (Figure 10a), *m/z* 341 (Figure 10b), and *m/z* 327 (Figure 10c); and molecular ion peaks at *m/z* 464 (Figure 10a), *m/z* 356 (Figure 10b), and *m/z* 342 (Figure 10c). Another possible fragmentation route is the loss of $H_2C{=}Si(CH_3)_2$ (72 u) from the silylated site of the analytes, giving rise to product ions at *m/z* 392, 284, and 270 for SARM A, B, and C, respectively. Since APPI and EI both produce $M^{+\bullet}$ ions, similar ions would be expected in APPI-MS/MS and EI-MS spectra, and were in fact observed. The resemblance of the mass spectra is clearly seen in a comparison of the APPI-MS/MS spectra in Figure 10 with the EI-MS spectra in Figure 11. This similarity may be advantageous in analyte characterization since the APPI-MS/MS spectra of $M^{+\bullet}$ ions can be matched against the EI-MS spectral libraries.

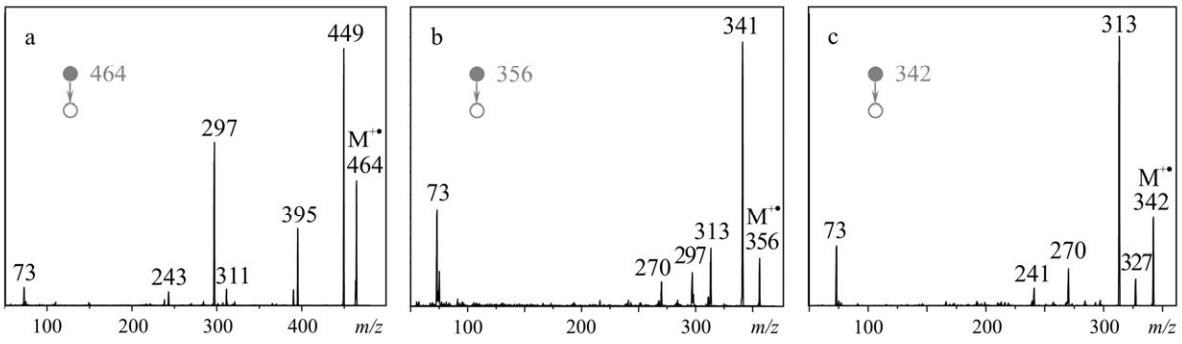

Figure 10 *MS/MS spectra of the $M^{+\bullet}$ ions of trimethylsilylated SARMs obtained from GC peaks with µAPPI. The spectra are the average spectra with different collision energies in the range 20–65 eV. (a) SARM A-TMS ($M^{+\bullet}$ ion at* m/z *464), (b) SARM B-TMS ($M^{+\bullet}$ ion at* m/z *356), and (c) SARM C-TMS ($M^{+\bullet}$ ion at* m/z *342).*

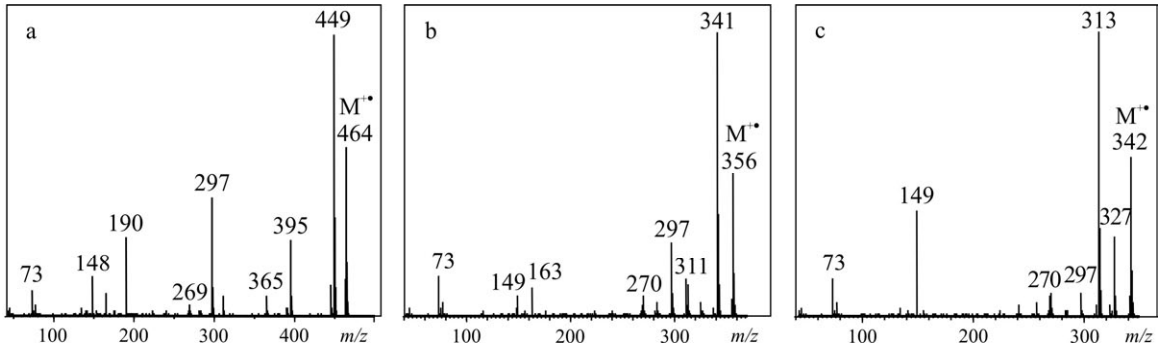

Figure 11 *EI-MS spectra of trimethylsilylated SARMs obtained from a GC-EI-MS run. (a) SARM A-TMS ($M^{+\bullet}$ ion at* m/z *464), (b) SARM B-TMS ($M^{+\bullet}$ ion at* m/z *356), and (c) SARM C-TMS ($M^{+\bullet}$ ion at* m/z *342).*

6.1.3 Performance of GC-µAPI-MS: analysis of PCBs

The analytical characteristics of GC-µAPI-MS – LODs, linear ranges, and repeatabilities – were determined from data obtained in the analysis of PCB standards. The values for each congener are presented in Table 7. The LODs for penta- to heptachlorinated congeners were at low picogram level (1-30 pg) with both GC-µAPCI-MS and GC-µAPPI-MS methods. PCB 28 and PCB 52 had relatively high LODs, which indicates that the methods are not very suitable for these congeners. The linearities and repeatabilities (see discussion below) for these compounds are not, therefore, presented. The slightly better LODs in µAPCI-MS than in µAPPI-MS may be due to the large size of the UV lamp holder relative to the corona discharge needle, which prevented the optimal positioning of the lamp and the API microchip. In negative ion APCI and APPI methods, the ionization efficiency, and thus the signal intensity, increases with the EA of the analyte [138]. Since highly chlorinated congeners have higher EAs than less chlorinated ones, the methods are most suitable for congeners with more than four chlorine substituents. Similar trends of increasing response with increasing number of chlorines have been reported in negative CI-MS [139] and ECD [140]. Although, in general, an increase in the degree of chlorination increases the signal of the analyte, chlorine substituents in ortho positions decrease the response as compared with congeners that have the same number of chlorine atoms but not in ortho position [138,141,142]. In the present study, the phenomenon is most pronounced for PCB 52, which gives lower response than PCB 28. Congener PCB 52 is tetrachlorinated and has two ortho chlorines, whereas PCB 28 is trichlorinated and has only one ortho chlorine. According to these findings, negative ion µAPCI and µAPPI methods are best suited for the analysis of highly chlorinated, or non-ortho or mono-ortho PCBs. Such congeners are also the most toxic and thus the most interesting ones in environmental samples. For the analysis of less chlorinated, lower EA congeners, positive ion mode might be more suitable than negative, as has been reported for other halogenated compounds with conventional APPI-MS [35] and positive CI-MS [140]. To investigate this, positive ion APPI was tested for the PCBs of this study at concentration levels of 30–500 ng/mL, which correspond to 30–500 pg on-column. In the case of PCB 28, $M^{+\bullet}$ ions were detected with LOD of 50 pg, which is lower than the LOD value in negative ion mode (200 pg). The remaining compounds produced no signal at all in positive ion mode.

The R^2 values (Table 7) were similar in the two setups studied, but the linear ranges were slightly wider with APPI (from LOD levels up to 3000 pg; 3000 ng/mL solution with 1 µL injection volume) than with APCI (from LOD levels up to 1000 pg; 1000 ng/mL solution with 1 µL injection volume). However, the difference is small and probably insignificant, especially since in previous comparisons of the linear ranges of APCI and APPI the results have been inconsistent [143-146].

The repeatabilities (RSD%) of the two methods were at acceptable levels (RSD: 12-33% with APCI, and 10-15 % with APPI) (Table 7). The probable reason for the variation of the peak areas is the combination of narrow GC peaks (w_h = 3 s), and the relatively slow MS acquisition rate of the ion trap MS. The better repeatability with APPI than with APCI may be due to the greater stability of the UV lamp radiation than corona discharge as the producer of ionizing electrons: the corona discharge current in negative ion APCI consists of tiny pulses [147], which may cause instability, seen as fluctuation of the signal.

The analytical characteristics of GC-µAPCI-MS and GC-µAPPI-MS cannot reasonably be compared with those of conventional GC-MS systems since combinations of GC with APPI-MS [45,54] and APCI-MS [55] are rarely used. However, the LODs for

mono- to pentachlorobiphenyls have been reported to be approximately 50 pg in an online system with gaseous samples and negative corona discharge ionization [148]. In another study [149] the LODs in negative corona APCI were from a few pg to hundreds of pg (estimated from µg/Nm^3 online monitoring values). The LODs obtained in the present study are in the same range as those.

Table 7. *LODs, linearities, and repeatabilities for PCBs with photoionization (µAPPI) and corona discharge ionization (µAPCI).*

Congener	LOD‡ (pg)		Linearity (R^2)		Repeatability§ (RSD %)	
	µAPCI	µAPPI	µAPCI*	µAPPI†	µAPCI	µAPPI
PCB 28	100	200	-	-	-	-
PCB 52	1000	2000	-	-	-	-
PCB 101	30	30	0.999	0.998	22	13
PCB 118	10	10	0.997	0.997	12	10
PCB 153	10	30	0.997	0.998	33	14
PCB 138	1	1	0.990	0.998	15	14
PCB 180	10	30	0.999	0.999	21	15

‡ S/N>3.
* Linear ranges from LODs to 1000 pg (1000 ng/mL solution with 1 µL injection volume). Individual data points in regression are averages of five measurements.
† Linear ranges from LODs to 3000 pg (3000 ng/mL solution with 1 µL injection volume). Individual data points in regression are averages of three measurements.
§ 500 pg per injection with five measurements.

Comparison of quantitation results obtained by GC-µAPPI-MS and GC-ECD

The feasibility of the GC-µAPPI-MS method in real-life analytics was investigated by analyzing five of the PCB congeners in authentic soil samples and comparing the results with values obtained by GC-ECD. The concentration values obtained by GC-µAPPI-MS (Table 8) were calculated from two replicates with external calibration in the range of 3–300 ng/ml. The results obtained by GC-ECD (Table 8), in the laboratory of the Finnish Environment Institute, were calculated with internal standard calibration (PCB 53, 94.4 ng/ml and tetrachloronaphthalene, 36.6 ng/ml). Extracts 1 and 2 represent two adjacent extractions from the same soil sample. The results are consistent and indicate that the GC-µAPPI-MS method can be utilized in quantitative analysis of environmental samples. The only notable deviation of the results was for PCB 138. The shape of the chromatographic peak of that congener obtained by GC-µAPPI-MS was not acceptable, perhaps due to some unknown compound that elutes from the column at the same time and suppresses the ionization of the analyte.

Table 8. *Concentrations of selected PCBs in soil samples (ng/ml) obtained with GC-µAPPI-MS and GC-ECD.*

Congener	GC-µAPPI-MS		GC-ECD	
	Extract 1 (ng/mL)	Extract 2 (ng/mL)	Extract 1 (ng/mL)	Extract 2 (ng/mL)
PCB 101	64	71	62	59
PCB 118	11	16	31	30
PCB 153	157	189	139	126
PCB 138	21	33	160	145
PCB 180	105	176	151	103

6.1.4 Performance of GC-µAPI-MS: analysis of SARMs

Two techniques, GC-µAPPI-MS (with triple quadrupole MS) and GC-µAPCI-Orbitrap MS, were studied in SARM analysis (**II**). The analytical characteristics of the GC-µAPPI-MS technique were studied in detail with derivatized analytes in urine, whereas the GC-µAPCI-Orbitrap MS technique was demonstrated at proof-of-concept level in the analysis of derivatized standard compounds.

GC-µAPPI-MS

The performance of GC-µAPPI-MS was evaluated with spiked urine samples. Before analysis the samples were hydrolyzed, extracted by SPE, and derivatized with N-methyl-N-(trimethylsilyl)trifluoroacetamide (MSTFA). Trimethylsilylated compounds were detected with three diagnostic SRM ion pairs per compound (Table 9). The method was shown to be selective in a comparison of the extracted ion chromatograms of the SRM ion pairs of a spiked urine sample with the chromatograms of a blank urine sample (Figure 8). The LODs and the limits of quantitation (LOQs) were determined for single SRM ion pairs (Table 1). LODs for SARMs in urine were in the range of 0.01–1 ng/mL with S/N≥3, and LOQs in the range 0.03–3 ng/mL with S/N≥10. In a previous study with LC-ESI-MS, the LODs for non-derivatized 2-quinolinone-derived SARMs in urine were reported to be in the range of 0.01–0.2 ng/mL [121], and in a study with GC-EI-MS the LOD was 0.2 ng/mL for trimethylsilylated SARM A [122]. The World Anti-Doping Agency's minimum required performance level for an anabolic agent is 2 or 10 ng/mL in urine, depending on the compound [150]. Our method meets the requirements, especially in the case of the most potent [151,152] and most interesting compound, SARM A, also known as the drug candidate LGD-2226. Two reasons can be suggested for the excellent sensitivity for SARM A: the compound is effectively ionized due to its high fluorine content, and its $M^{+\bullet}$ ions appear at higher mass range than the background compounds in urine. The mass spectrometric response of the analytes was linear (R≥0.995, with 1/x weighting, 4-8 concentration levels in a regression) from the LOQ concentration level up to 100 ng/mL concentration. The relative standard deviation of the peak areas in the SRM chromatograms was low (5–9%) for all compounds (Table 9). In addition, the extraction recovery percentages (92–111%) are acceptable and show only slight variation (2–6%) for three replicates of each compound. In view of these characteristics, the method is concluded to show potential for quantitative analysis. In doping analysis, however, qualitative analysis is often sufficient.

Table 9. *Monitored SRM ion pairs from $M^{+\bullet}$ and $[M+H]^+$ precursor ions of trimethylsilyl derivatized SARMs. The quantitative ion pair for $M^{+\bullet}$ ions is shown in bold. Limits of detection (LODs) (S/N ≥ 3), limits of quantitation (LOQ) (S/N ≥ 10), intra-day repeatabilities, and extraction recoveries are for $M^{+\bullet}$ ions.*

	Diagnostic ion pairs and **quantitative ion pair** from $M^{+\bullet}$ (*m/z*)	Diagnostic ion pairs from $[M+H]^+$ (*m/z*)	LOD; *LOQ* (ng/mL in urine) [a]	Peak area repeatability (RSD%) [b]	Retention time repeatability (RSD%) [b]	Recovery in SPE (%) [c]
SARM A-TMS	464/449 464/395 **464/297**	465/449 465/297 465/73	0.01; *0.03*	7	0.03	92 ± 3
SARM B-TMS	**356/341** 356/313 356/297	357/341 357/311 357/297	1; *3*	5	0.04	102 ± 6
SARM C-TMS	**342/313** 342/270 342/241	343/327 343/285 343/257	0.1; *0.3*	9	0.05	111 ± 2

[a] For $M^{+\bullet}$ ions.
[b] Averages of three concentration levels of SARMs in urine (three replicates at each level):
SARM A-TMS: 0.1, 3, and 30 ng/mL
SARM B-TMS: 3, 10, and 30 ng/mL
SARM C-TMS: 1, 3, and 30 ng/mL
[c] Average of three replicates. SARM concentrations: 3 ng/mL in urine.

Proof-of-concept of GC-µAPCI-Orbitrap MS technique

The selectivity and thus the analytical performance of the analysis method for SARMs can be enhanced by using an MS with high resolving power. The combination of GC-µAPI with such an instrument, Orbitrap MS, was demonstrated. APCI was used for the ionization, and the formation of $[M+H]^+$ ions was clearly observed. EICs of the $[M+H]^+$ ions with *m/z* window of 0.03 u for trimethylsilylated SARMs from a GC-µAPCI-Orbitrap MS run are presented as an example of the results (Figure 12). The reduced background interference when accurate masses are used for extraction of the ion chromatograms is demonstrated. Excellent agreement was achieved between the measured and calculated masses (mass error <2 ppm): the measured masses of SARMs A, B, and C were *m/z* 465.1048, 357.1611, and 343.1453, whereas the calculated masses were *m/z* 465.1045, 357.1610, and 343.1453, respectively.

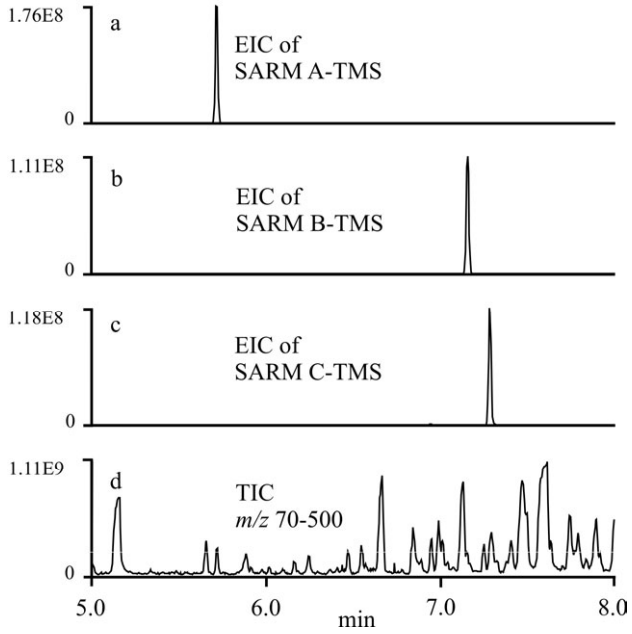

Figure 12 *Extracted ion chromatograms (EIC) of the three trimethylsilylated SARMs and a total ion chromatogram (TIC) from a GC-µAPCI-Orbitrap MS run. (a) EIC at mass range* m/z *465.09–465.12, (b) EIC at mass range* m/z *357.15–357.18, (c) EIC at mass range* m/z *343.13–343.16, and (d) TIC at mass range* m/z *70–500. Concentration of non-derivatized analytes is 10 µg/mL and injection volume 1 µL (splitless injection).*

6.2 DAPPI-MS

This section summarizes the research on DAPPI-MS presented in Papers **III**, **IV**, and **V**. The first task was to study the ion source configuration and desorption/ionization (D/I) mechanisms in DAPPI (**III**). The ion source parameters were investigated in two different configurations (orthogonal and parallel), and the D/I mechanisms were studied by testing the suitability of various spray solvents for different types of analytes, and comparing the performances of sample plate materials with different thermal and electrical conductivities and surface porosities. Ionization in DAPPI in positive (**III**, **IV**, **V**) and negative (**III**, **IV**) ion modes was then studied with compounds of different physicochemical properties. Finally, DAPPI-MS methods were applied in the rapid screening analysis of harmful compounds in environmental and food samples (**IV**) and confiscated drugs (**V**), and the performance of DAPPI was compared with that of DESI (**V**).

6.2.1 Ion source configuration

MS parameters, positioning of the API microchip and positioning of the sample spot relative to the MS inlet and the API microchip were optimized (for details see Paper **III**). The distances x and y of the sample spot from the MS inlet and the angle between the nebulizer microchip and the sample plate (Figure 13) were optimized to give maximum intensity of the analyte signal. With proper positioning, both orthogonal and parallel configurations of the DAPPI microchip plume worked well. However, adjusting the position of the sample spot relative to the plume of the vaporized spray solvent and the MS inlet was less complicated with the parallel setup, so that it produced a more repeatable signal. In the analysis of concentrated samples (i.e., tablets) more contamination and memory effect were associated with the parallel setup than the orthogonal setup since the plume of the nebulizer chip was directed towards the MS inlet. The orthogonal configuration is therefore recommended for the analysis of samples with high analyte concentration. Since contamination was not an issue with our diluted samples, however, the parallel setup was used in the rest of the experiments.

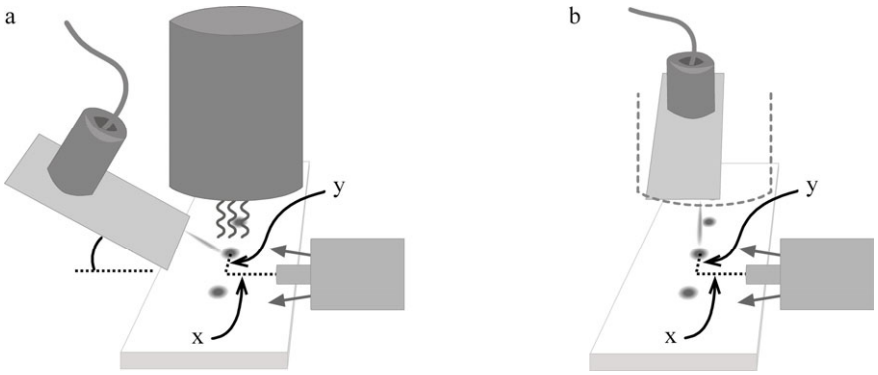

Figure 13 *Parallel (a) and orthogonal (b) experimental setups in DAPPI. The heated jet desorbs the analytes from the surface, after which the analytes are ionized in gas phase by photons emitted by the krypton discharge lamp, and the analytes are finally introduced to the MS through a capillary extension. The x and y distances of the sample spot from the capillary extension tip and the angle between the microchip and the sampling surface were optimized. The optimal angle was 45º, and the optimal sample spot distances were x = 3 mm and y = 0 mm in the parallel setup (a) and x = 1 mm and y = 3 mm in the orthogonal setup (b). In (b) the position of the UV lamp is shown with a dashed line. In both configurations the sampling surface was placed very close (distance ~0.5 mm) to the MS capillary extension tip.*

6.2.2 Effect of spray solvent on analyte ionization

One objective of the work reported in Paper **III** was to determine the suitability of different organic solvents as spray solvents in DAPPI. Six solvents – acetone, anisole, hexane, methanol/toluene (50/50, v/v), 2-propanol, and toluene – were tested in the analysis of ten compounds. The ten compounds were anthracene, MDMA, BaP, testosterone, tetracyclone, and verapamil in positive ion mode and 1,4-dinitrobenzene, 2-naphthoic acid, 1,4-naphthoquinone, and paracetamol in negative ion mode (Figure 3). Poly(methyl methacrylate) (PMMA) sample plates were used as sampling surfaces since the analyte signal from PMMA plates was relatively high and repeatable.

The ionization reactions in DAPPI are similar to those in APPI (section 2.1) except that unlike in most reported cases with APPI, the only solvent present is the spray solvent (i.e., there is no mobile phase from LC). Thus, with one exception, the reactant ions were formed solely from the spray solvent (marked as "D" in section 2.1) and atmospheric gases. The exception was where methanol/toluene was used as the spray solvent and methanol reacted with the radical cation of toluene (reaction 29, section 2.1).

Positive ion mode

In positive ion mode, the spray solvent affected the analyte ion composition and the analyte ion intensity (Figure 14a). With anisole or toluene as the spray solvent, the nonpolar compounds anthracene, BaP, and tetracyclone formed mainly $M^{+\bullet}$ ions by charge exchange (reaction 22, section 2.1) (Figure 14a). With hexane or methanol/toluene (50/50, v/v) as the spray solvent, BaP and tetracyclone produced $[M+H]^+$ ions, formed by proton transfer (reactions 24 and 30, section 2.1). With acetone and 2-propanol, only tetracyclone was ionized, forming $[M+H]^+$ ions by proton transfer. The polar compounds MDMA, testosterone, and verapamil produced $[M+H]^+$ ions with all spray solvents. However, when

anisole or toluene was used, the mass spectrum of verapamil was dominated by the fragment ion peak $[M\text{-}C_9H_{11}O_2]^+$ at *m/z* 303 rather than the $[M+H]^+$ ion at *m/z* 455.

Anisole and toluene both have relatively low IEs (Table 10) and easily form radical cations (reaction 21, section 2.1), which react through charge exchange with analytes to produce $M^{+\bullet}$ analyte ions if the IE of the analyte is lower than that of the solvent (reaction 22, section 2.1). Thus, analytes with relatively low IEs (anthracene, BaP, and tetracyclone) produce radical cations, $M^{+\bullet}$, when anisole or toluene is used as spray solvent. If the analyte has a higher PA than the spray solvent, however, reactant ions originating from the solvent donate protons to the analytes (MDMA, testosterone, and verapamil) to produce protonated molecular ions, $[M+H]^+$ (reactions 24 and 30, section 2.1). Acetone, 2-propanol, methanol, methanol/toluene, and hexane produce proton-donating reactant ions by self-protonation, and except for anthracene, which has low PA, $[M+H]^+$ ions are observed with these solvents as the result of proton transfer reactions. Of the nonpolar compounds, the PA of BaP (887 kJ/mol [153]) is higher than that of anthracene (877 kJ/mol [33]) due to the larger number of conjugated carbon rings in the molecular structure and thus greater number of delocalized π-electrons. Therefore, $[M+H]^+$ ions were seen in the spectrum of BaP but not that of anthracene.

Toluene and acetone were selected as spray solvents in the further studies in positive ion mode (**IV**, **V**) since toluene exhibited good overall ionization efficiency for neutral, nonpolar compounds, and acetone for compounds with high PA (Figure 14a). Although anisole performed well in the analysis of nonpolar compounds, it was excluded to keep the experimental setup simple.

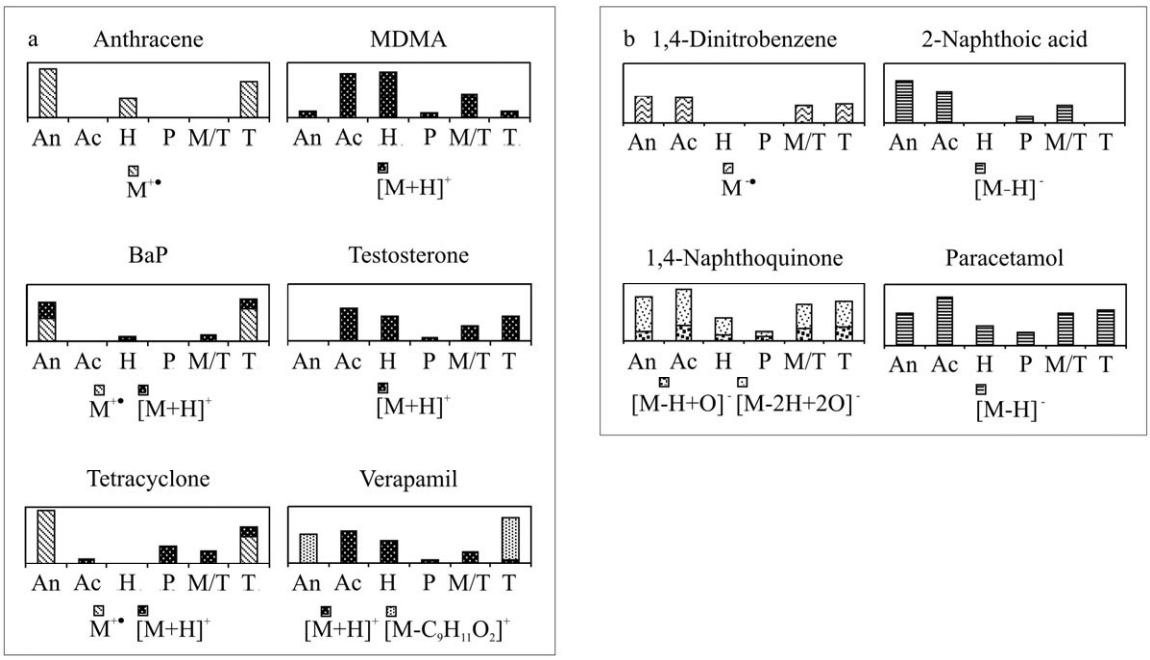

Figure 14 *Average signal intensities of the analyte ions with six different spray solvents in (a) positive and (b) negative ion mode DAPPI. All the samples were applied on a PMMA surface. Spray solvents: An: anisole, Ac: acetone, H: hexane, P: 2-propanol, M/T: methanol/toluene (50/50, v/v), and T: toluene. For conditions see Paper* ***III****.*

Negative ion mode

In negative ion mode, the same ions were produced with all the spray solvents (Figure 14b). The spectrum of 1,4-dinitrobenzene, which has positive EA (2.00 eV [33]), showed $M^{-\bullet}$ ions formed by electron capture (reaction 14, section 2.1) or charge exchange with superoxide radical (reaction 13, section 2.1). 1,4-Naphthoquinone produced $[M-H+O]^-$ and $[M-2H+2O]^-$ ions. Formation of these kinds of oxidization products from substituted aromatic compounds (reactions 16 and 17, section 2.1) in negative atmospheric pressure ionization has been reported on several occasions, such as from chlorobenzenes [32], chloronitrobenzenes [32,34], polychlorinated biphenyls [32], polybromodiphenylethers [35] and 1,4-naphthoquinone [36]. The acidic compounds naphthoic acid and paracetamol produced $[M-H]^-$ ions, formed through proton transfer to the superoxide radical (reaction 15, section 2.1) or another reactant ion.

With the solvents and analytes studied in negative ion mode, the type of solvent affected only the intensity of the analyte ion signal, not the type of ions formed (Figure 14b). The ionization mechanism is proposed to be determined by the EA and gas-phase acidity of the analyte and the spray solvent (Table 10) and the signal intensity by the amount of ionizing electrons. The latter depends on the IE of the spray solvent, and the ionization is less efficient with high IE solvents (hexane and 2-propanol), than with low IE solvents (anisole, acetone, and toluene), as can be seen in the analyte signal intensities of Figure 14b. If the ionization energy of the spray solvent is in the range 10.0–10.6 eV, the majority of photons emitted by the krypton discharge lamp (with 10 eV energy) are incapable of ionizing the solvent, and ionization is initiated only by the minority 10.6-eV photons. Methanol is not ionized by the UV lamp since its IE is 10.8 eV, but it forms reactant ions in the reaction with toluene (reaction 29, section 2.1).

Since anisole produced both high analyte signal intensity and low background, it was selected as spray solvent in the further studies in negative ion mode (**IV**).

Table 10. *Properties of the spray solvent and gases* [33].

Spray solvent	IE (eV)	PA (kJ/mol)	Gas-phase acidity, ΔG_{acid} (kJ/mol)
Acetone	9.7	812	1515
Anisole	8.2	840	1648
Hexane	10.1		
Methanol	10.8	754	1565
2-Propanol	10.2	793	1543
Toluene	8.8	784	1567
Nitrogen	15.6	494	
Oxygen	12.1	421	
$HO_2^{\bullet}$			1451

6.2.3 Observed analyte ions

Study was made of the ionization of compounds of different physicochemical properties (**III**, **IV**, and **V**). The observed ions, together with the spray solvents used, are listed in Table 11. The compounds discussed in section 6.2.2 (in regard to the effect of the spray solvent on the analyte ionization) are included in the listing.

Positive ion mode

Most of the analytes showed either $M^{+\bullet}$ or $[M+H]^+$ ions, or both, in their mass spectra, and some of them also fragment or adduct ions (Table 11). $M^{+\bullet}$ ions alone were observed in the mass spectra of anthracene, BkF, chrysene, phenanthrene, and TBBPA. Both $M^{+\bullet}$ and $[M+H]^+$ ions were formed from BaP, caffeine, carbofuran, cocaine, heroin, imazalil, methiocarb, phenacetine, pirimicarb, tetracyclone and thiabendazole. The compounds that formed no $M^{+\bullet}$ ions, but instead $[M+H]^+$ ions, were acridine, amphetamine, ditalimfos, MDMA, methamphetamine, methomyl, testosterone and verapamil. Some analytes (aldicarb and oxamyl) showed only fragment or adduct ions in their mass spectra.

Charge exchange reaction, leading to the formation of $M^{+\bullet}$ ions (reaction 22, section 2.1), occurs when IE of the analyte is lower than that of the spray solvent and the PA of the analyte is low, as often is the case with neutral and nonpolar compounds. When the PA of the analyte is higher than that of the spray solvent, the analyte is ionized by proton transfer (reactions 24 and 30, section 2.1), which is the ionization mechanism in the case of basic compounds. Many analytes produced both $M^{+\bullet}$ and $[M+H]^+$ ions (Table 11), evidently due to low IE and relatively high PA of the analyte. In addition, the properties of the spray solvent affect the type of analyte ions (see section 6.2.2). Formation of fragment and adduct ions was observed with many analytes (Table 11), but the factors affecting the formation were not studied.

Negative ion mode

Formation of $M^{-\bullet}$ ions was observed for 1,4-dinitrobenzene, and $[M-H]^-$ ions for 2-naphthoic acid, paracetamol, TBBPA, and thiabendazole; 1,4-naphthoquinone produced $[M-H+O]^-$ and $[M-2H+2O]^-$ ions; and imazalil produced $[M-Cl+O]^-$ ions (Table 11). In addition, fragment ions were formed from some compounds (imazalil, methiocarb, and oxamyl).

The formation of $M^{-\bullet}$ ions (reactions 13 and 14, section 2.1) from neutral, nonpolar 1,4-dinitrobenzene is due to the high EA of the compound (2.00 eV [33]). Deprotonation reaction between the analyte and superoxide ion ($O_2^{-\bullet}$) leading to the formation of $[M-H]^-$ ions (reaction 15, section 2.1) occurs when the gas-phase acidity of an analyte is higher than that of the $HO_2^\bullet$ radical. This is the case with acidic analytes: 2-naphthoic acid, paracetamol, TBBPA, and thiabendazole (for example, ΔG_{acid} for 2-naphthoic acid is 1370 kJ/mol, and that for $HO_2^\bullet$ radical 1450 kJ/mol). Formation of phenoxide ions has been observed for several substituted aromatic compounds in API when oxygen is present in the ion source [32,34-36]. In the present study, phenoxide ions were formed from 1,4-naphthoquinone ($[M-H+O]^-$ and $[M-2H+2O]^-$) and imazalil ($[M-Cl+O]^-$) (reactions 16 and 17, section 2.1). The formation of fragment ions was observed for imazalil, methiocarb, and oxamyl but was not studied.

Table 11. *Ions observed in DAPPI-MS with different spray solvents (given in parenthesis): Ac, acetone; An, anisole; H, hexane; MT, methanol/toluene (50/50, v/v); P, 2-propanol; and T, toluene. Not all spray solvents were tested for all compounds. "n.d." means not detected, "-" means not tested. For details see the original publications.*

Compound ($M_{monoisotopic}$ (g/mol))	Positive ion mode	Negative ion mode	Paper
Acridine (179.07)	$[M+H]^+$ (Ac, T)	n.d. (An)	IV
Aldicarb (190.08)	$[M-CH_3NHCOO]^+$ (Ac, T) $[M-27]^+$ (T) $[M+47]^+$ (Ac, T) $[2M+H]^+$ (Ac, T)	n.d. (An)	IV
Amphetamine (135.10)	$[M+H]^+$ (Ac, T)	-	V
Anthracene (178.08)	$M^{+\bullet}$ (An, H, T) n.d. (Ac, P, MT)	-	III
BaP (252.09)	$M^{+\bullet}$ (An, T) $[M+H]^+$ (An, H, MT, T) n.d. (Ac, P)	n.d. (An)	III, IV
BkF (252.09)	$M^{+\bullet}$ (T) n.d. (Ac)	n.d. (An)	IV
Caffeine (194.08)	$M^{+\bullet}$ (T) $[M+H]^+$ (Ac)	-	V
Carbofuran (221.11)	$M^{+\bullet}$ (T) $[M+H]^+$ (Ac, T) $[M+H-CH_3NHCO]^+$ (T) $[2M+H-CH_3NHCO]^+$ (T)	n.d. (An)	IV
Chrysene (228.09)	$M^{+\bullet}$ (T) n.d. (Ac)	n.d. (An)	IV
Cocaine (303.15)	$M^{+\bullet}$ (T) $[M+H]^+$ (Ac, T)	-	V
1,4-Dinitrobenzene (168.02)	-	$M^{-\bullet}$ (Ac, An, MT, T)	III
Ditalimfos (299.04)	$[M+H]^+$ (Ac, T) $[M-136]^+$ (Ac, T) $[M+33]^+$ (Ac, T)	n.d. (An)	IV
Heroin (369.16)	$M^{+\bullet}$ (T) $[M+H]^+$ (Ac, T)	-	V
Imazalil (296.05)	$M^{+\bullet}$ (T) $[M+H]^+$ (Ac, T) $[M+H-CH_2CHCH_2O]^+$ (T) $[M-Cl]^+$ (T)	$[M-Cl+O]^-$ (An) $[M-Cl+O-CH_2CHCH_2O]^-$ (An)	IV
MDMA (193.11)	$[M+H]^+$ (Ac, An, H, P, MT, T)	-	III, V
Methamphetamine (149.12)	$[M+H]^+$ (Ac, T)	-	V
Methiocarb (225.08)	$M^{+\bullet}$ (T) $[M+H]^+$ (Ac, T) $[M-CH_3NCO]^+$ (T) $[M+H-CH_3NCO]^+$ (Ac) $[2M+H]^+$ (Ac)	$[M-H-CH_3NCO]^-$ (An)	IV
Methomyl (162.05)	$[M+H]^+$ (Ac, T) $[2M+H]^+$ (Ac, T) $[M+H-CH_3NHCOO]^+$ (T)	n.d. (An)	IV
Naphthalene (128.06)	n.d. (Ac, T)	n.d. (An)	
2-Naphthoic acid (172.05)	-	$[M-H]^-$ (Ac, An, P, MT)	III
1,4-Naphthoquinone (158.04)	-	$[M-H+O]^-$ (Ac, An, H, P, MT, T) $[M-2H+2O]^-$ (Ac, An, H, P, MT, T)	III
Oxamyl (219.07)	$[(CH_3)_2NCO]^+$ (Ac, T) $[M+H-(CH_3)_2NCO-CH_3NHCO]^+$ (Ac, T) $[M+H-CH_3NCO]^+$ (Ac, T) $[2M+H-CH_3NCO]^+$ (Ac, T) $[2M+H]^+$ (Ac, T)	$[M-58]^-$ (An) $[M-25]^-$ (An)	IV
Paracetamol (151.06)	-	$[M-H]^-$ (Ac, An, H, P, MT, T)	III
Phenacetine (179.09)	$M^{+\bullet}$ (T) $[M+H]^+$ (Ac)	-	V

Compound ($M_{monoisotopic}$ (g/mol))	Positive ion mode	Negative ion mode	Paper
Phenanthrene (178.08)	$M^{+\bullet}$ (T) n.d. (Ac)	n.d. (An)	IV
Pirimicarb (238.14)	$M^{+\bullet}$ (T) $[M+H]^+$ (Ac, T) $[M-(CH_3)_2NCO]^+$ (T)	n.d. (An)	IV
Testosterone (288.21)	$[M+H]^+$ (Ac, H, P, MT, T) n.d. (An)	-	III
TBBPA (539.76)	$M^{+\bullet}$ (T) n.d. (Ac)	$[M-H]^-$ (An)	IV
Tetracyclone (384.15)	$M^{+\bullet}$ (An, T) $[M+H]^+$ (Ac, P, MT, T)	-	III
Thiabendazole (201.04)	$M^{+\bullet}$ (T) $[M+H]^+$ (Ac, T)	$[M-H]^-$ (An)	IV
Verapamil (454.28)	$[M+H]^+$ (Ac, H, P, MT, T) $[M-C_9H_{11}O_2]^+$ (An, T)	-	III

Abbreviations for analytes in Table 11:

BaP	Benzo[a]pyrene
BkF	Benzo[k]fluoranthene
MDMA	3,4-Methylenedioxymethamphetamine
TBBPA	Tetrabromobisphenol A

6.2.4 Sample plate materials

Several materials have been introduced as sampling surfaces in desorption ionization techniques [8,154-156], and the choice of sampling surface has been reported to significantly affect sensitivity and selectivity in DESI. The effect of different sample surface materials on the analyte signal intensity in DAPPI was investigated in the present study (**III**).

Ten sample plate materials with different thermal conductivity, surface porosity, and thickness were studied: aluminum (thickness 3 mm), aluminum foil (thickness 15 µm), copy/print paper, filter paper, microscope glass slide, kitchen paper, PMMA, poly(tetrafluoroethylene) (PTFE), silicon (thickness 0.5 mm), and thin-layer chromatography (TLC) plate. Based on preliminary tests with these materials, six materials were chosen for further study: aluminum, aluminum foil, copy/print paper, glass, PMMA, and PTFE. Ten test compounds (anthracene, BaP, 1,4-dinitrobenzene, MDMA, 2-naphthoic acid, 1,4-naphthoquinone, paracetamol, testosterone, tetracyclone, and verapamil) were desorbed from these six surfaces. Spray solvents chosen for the sampling surface study were as follows: acetone was used for polar compounds in positive ion mode since it showed the best overall ionization efficiency for polar compounds (Figure 14a); toluene was used for nonpolar compounds in positive ion mode in view of its ability to produce both $M^{+\bullet}$ and $[M+H]^+$ ions (Figure 14a); and anisole was used for all compounds in negative ion mode since it produced high analyte signal intensity (Figure 14b) and low background.

PMMA and PTFE were the best sample plate materials for all analytes studied (Figure 15), with sampling more repeatable from PMMA than from PTFE, probably because drifting of the sample droplets on the PTFE surface before drying complicated adjustment of the sample spot for the DAPPI-MS analysis. The other thermal insulators, glass and paper, worked fairly well in positive ion mode but performed poorly in negative ion mode. The sample droplets spread more on glass and paper than on PMMA and PTFE and the narrow and confined jet from the microchip was probably unable to desorb the entire

sample at once. Performance was better for the aluminum foil than the thick aluminum sample plate but, on the whole, poorer for these metal substrates than for the polymer substrates.

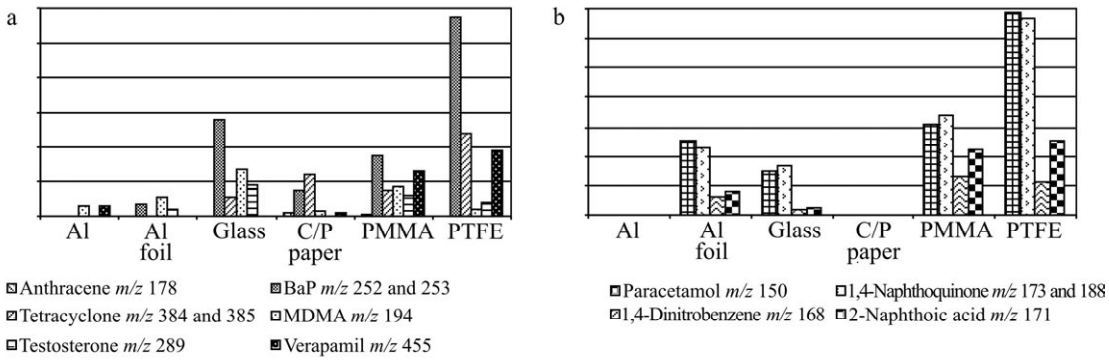

Figure 15 *Average analyte signal intensities from different sampling surfaces (aluminum (Al), aluminum foil (Al foil), microscope glass slide (Glass), copy/print paper (C/P paper), poly(methyl methacrylate) (PMMA) and poly(tetrafluoroethylene) (PTFE)) in (a) positive and (b) negative ion mode. Spray solvents in positive ion mode: toluene for nonpolar compounds (anthracene, benzo[a]pyrene, and tetracyclone) and acetone for polar compounds (MDMA, testosterone, and verapamil). Spray solvent in negative ion mode: anisole.*

Reactant ions appearing in the spectra were the same for all sampling surface materials, indicating that the surface material did not take part in the ionization process. Instead, differences in the ionization efficiencies were thought to depend on physical factors. Aluminum foil was an exception in showing relatively better performance in negative ion mode than in positive ion mode. As has been proposed in APPI [43] this may be due to the ability of the metal surface to release electrons and strengthen the ionization in negative ion mode. The polymer plates were assumed to work best because of their low thermal conductivity, which allows the spray solvent plume more efficiently to heat the sample spot. This hypothesis was supported by the better performance of the aluminum foil than of the thick aluminum plate. Further in support of the thermal nature of the desorption small molecules (with low boiling points) were observed to desorb faster than larger molecules (i.e., MDMA > testosterone > verapamil).

Local heating of the surface was further studied by thermal imaging [137] of selected sampling surfaces under the microchip plume. The thermographs in Figure 16 illustrate the sampling surface temperatures after 15 s of heating with the vapor plume. The differences between the materials with low (PMMA, kitchen paper) and high (aluminum foil, silicon) thermal conductivity are clearly seen. Because of their lower thermal conductivity, the polymer plates can be locally heated up to 300 ºC, and heating to high temperature seems to be an important factor for the effective desorption of the analytes in DAPPI. Figure 16a displays a hot spot on the PMMA sample plate, whereas Figure 16b shows the heat on the aluminum foil, with its better thermal conductivity, to be more widely and evenly spread. Kitchen paper can be locally heated up to 300 ºC with DAPPI, as shown in Figure 16c, but on silicon (Figure 16d) the hot spot is barely visible and, instead, the whole silicon sample plate is slightly heated. This result and the signal

intensities of the analytes from the different sampling materials support the conclusion that the desorption efficiency in DAPPI is dependent on the thermal conductivity of the surface.

It should be noted that the thermal imaging was carried out without heated drying-gas flow from the mass spectrometer (Figure 2), which would have affected the absolute temperatures of the sample plate and the ionization zone. The differences between the sampling materials were nevertheless clear. The effect of the specific heat capacity of the solvent was checked by thermal imaging with three spray solvents: water/methanol (50/50, v/v), toluene, and acetone. The type of solvent had no detectable effect on the heating rate or the final temperature of the sample plate.

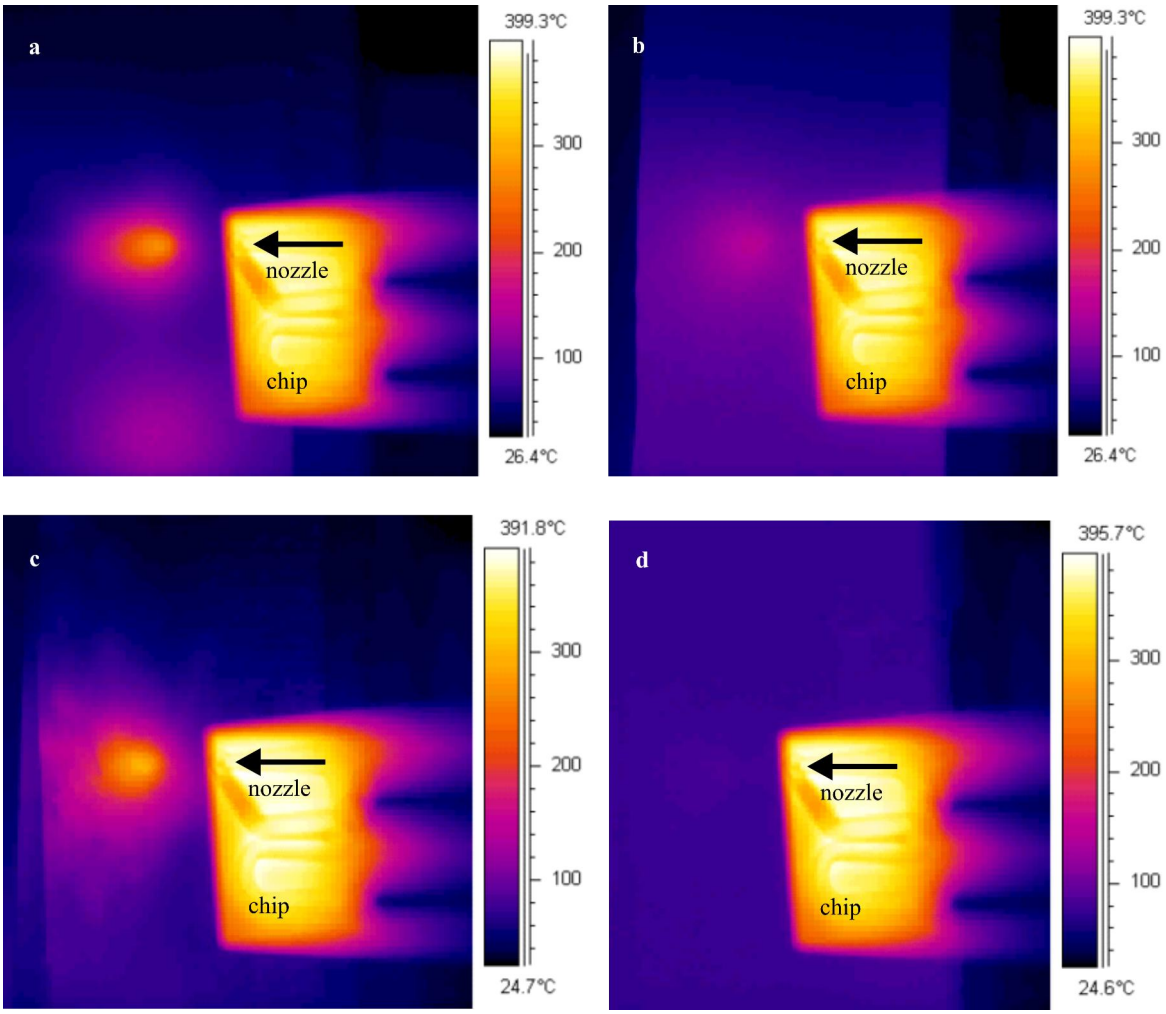

Figure 16 *Infrared thermography images of sample plates after 15 s of heating with the heated microchip plume. The sampling surfaces and the microchip (see Figure 2 for schematic view) are depicted from above. The chip heating power was 4.5 W, acetone was used as the spray solvent, and the nebulizer gas (nitrogen) flow rate was 180 mL/min. (a) PMMA (thickness 3 mm), T_{max} ~300 ºC, (b) aluminum foil (thickness 15 µm) on PMMA, T_{max} ~180 ºC, (c) kitchen paper on PMMA, T_{max} ~300 ºC, and (d) silicon (thickness 0.5 mm), T_{max} < 100 ºC. On PMMA (a), the second warm spot, below the spot being sprayed, is the position where the jet was directed before the recording.*

6.2.5 Applications

Authentic samples – circuit board (**V**), fruit peel (**V**), and illicit drug powders (**IV**) – and soil spiked with PAHs (**V**) were analyzed by DAPPI-MS to demostrate the feasibility of the methods in rapid screening analysis. For comparison, the drug samples were also analyzed by DESI-MS, which is widely reported in pharmaceutical and forensic analysis. Sampling procedures depended on the sample form; solid samples (circuit board, orange peel, and spiked soil pellet) were analyzed as such, whereas dissolved samples (illicit drugs) were analyzed from a dried droplet (diameter approx. 2 mm) on a PMMA sampling surface. In the former case, an area approx. 5 mm x 5 mm was scanned with the DAPPI plume, and in the latter case four replicate spots were analyzed. All the applications are discussed below, and Table 12 summarizes the analytes detected in samples. These applications in environmental, food, and forensic analysis demonstrate the feasibility of DAPPI-MS for rapid screening analysis of authentic samples. More accurate evaluation of the analytical performance of DAPPI-MS was done by determining the LODs for selected compounds. These are presented in section 6.2.6.

Table 12. *Samples, detected compounds, and observed ions in analyses by DAPPI-MS and DESI-MS. The DAPPI spray solvent is given in parenthesis: Ac, acetone; An, anisole; and T, toluene. The DESI spray solvent was water/methanol (50/50, v/v) + 0.1 vol-% acetic acid. "-" means not analyzed.*

Sample	Compounds detected by DAPPI-MS	Compounds detected by DESI-MS
Circuit board	TBBPA, $[M-H]^-$ (An)	-
Orange peel	Imazalil, $[M+H]^+$ (Ac)	-
Spiked soil	BkF, $M^{+\bullet}$ (T) Chrysene, $M^{+\bullet}$ (T) Phenanthrene, $M^{+\bullet}$ (T)	-
Drug sample 1	Amphetamine, $[M+H]^+$ (Ac)	Amphetamine, $[M+H]^+$
Drug sample 2	Amphetamine, $[M+H]^+$ (Ac) MDMA $[M+H]^+$ (Ac, T)	MDMA $[M+H]^+$
Drug sample 3	Methamphetamine, $[M+H]^+$ (Ac)	Methamphetamine, $[M+H]^+$
Drug sample 4	Heroin, $M^{+\bullet}$ (T), $[M+H]^+$ (Ac, T)	Heroin, $[M+H]^+$
Drug sample 5	Cocaine, $M^{+\bullet}$ (T), $[M+H]^+$ (Ac, T)	Cocaine, $[M+H]^+$
Drug sample 6	Cocaine, $M^{+\bullet}$ (T), $[M+H]^+$ (Ac, T)	Cocaine, $[M+H]^+$
Drug sample 7	Amphetamine, $[M+H]^+$ (Ac, T)	Amphetamine, $[M+H]^+$
Drug sample 8	Heroin, $M^{+\bullet}$ (T), $[M+H]^+$ (Ac, T)	Heroin, $[M+H]^+$
Drug sample 9	Methamphetamine, $[M+H]^+$ (Ac, T)	Methamphetamine, $[M+H]^+$

Abbreviations for analytes in Table 12:
TBBPA Tetrabromobisphenol A
BkF Benzo[k]fluoranthene
MDMA 3,4-Methylenedioxymethamphetamine

Analysis of circuit board

A piece of circuit board was analyzed as such by negative ion DAPPI-MS with anisole as the spray solvent. The mass spectrum showed a typical bromine isotopic pattern of $[M-H]^-$ ions at *m/z* 539–547 (Figure 17). The masses of the ions in the full-scan mass spectrum, as well as those observed in the MS/MS spectrum, matched with those of the TBBPA standard (see Paper **IV**). Thus the DAPPI method is concluded to show potential for the analysis of BFRs in polymers such as used in electronics.

Analysis of orange peel

DAPPI-MS with acetone as the spray solvent was used in the analysis of orange peel. An intense ion was detected at m/z 297, with a distinctive ^{37}Cl isotopic peak at *m/z* 299 (Figure 18a). The ion was recognized as the $[M+H]^+$ ion of imazalil, which was further confirmed by MS/MS analysis and comparison of the MS/MS spectrum with that of imazalil standard (see Paper **IV**). Imazalil is a post-harvest fungicide extensively applied to control fungi on fruits and vegetables. It is an environmental toxin, which interferes with physiological mechanisms in humans (e.g., hormone synthesis [157] and enzyme activity [158]). A piece of peel from an organically produced orange was analyzed for comparison, and no imazalil was detected (Figure 18b). The DAPPI-MS method would, therefore, be well suited to the fast screening of fruits or other foodstuff for pesticides.

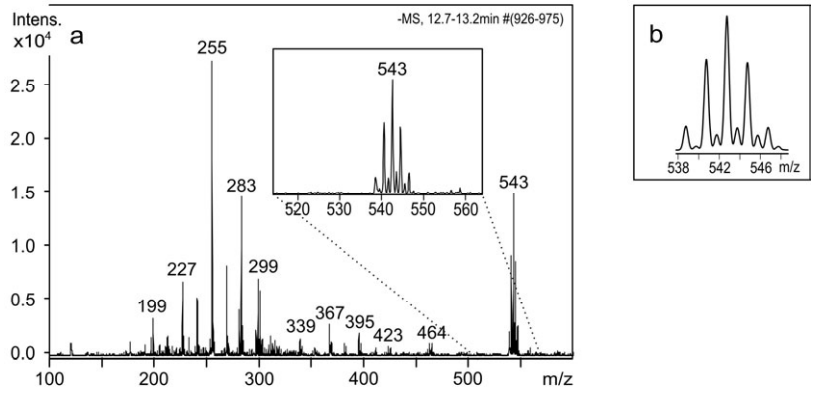

Figure 17 *(a) DAPPI mass spectrum obtained from a piece of circuit board in negative ion mode with anisole (10 µL/min) as the spray solvent. The isotopic pattern of the [M-H]⁻ ion of tetrabromobisphenol A is seen at* m/z *539–547. (b) Theoretical isotopic pattern of tetrabromobisphenol A.*

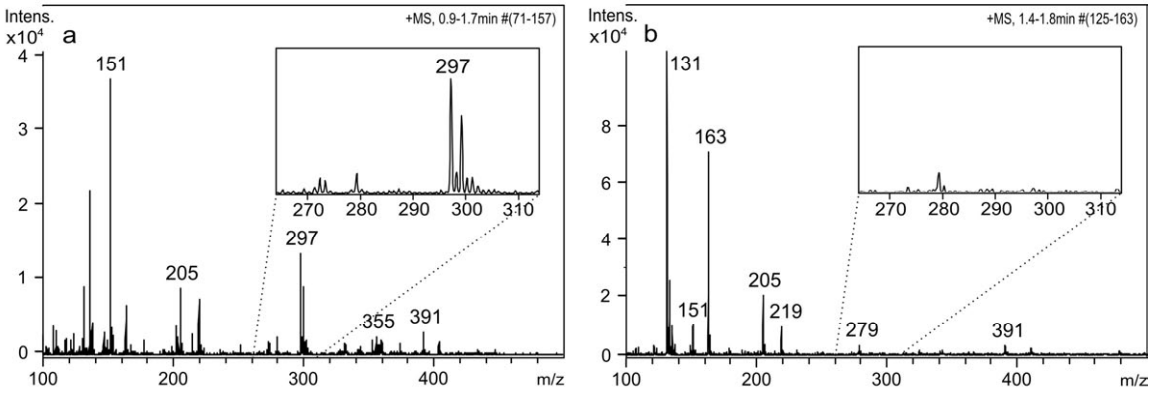

Figure 18 *The DAPPI mass spectra obtained from (a) normal orange peel and (b) peel from an organically produced orange in positive ion mode with acetone (10 µL/min) as the spray solvent. In a) the $[M+H]^+$ ion of imazalil is seen at* m/z *297 and the ^{37}Cl isotopic peak at* m/z *299.*

Analysis of soil spiked with PAHs

A soil pellet with high organic content, spiked with phenanthrene, chrysene, and BkF (10 µg/g of each in dry soil), was analyzed along with a blank soil pellet by DAPPI-MS with toluene as the spray solvent. The spiked compounds were chosen to represent PAHs of different molecular sizes and typical origins of pollution, such as vehicular emissions and incineration [159]. The mass peaks originating from the $M^{+\bullet}$ ions of phenanthrene, chrysene, and BkF are seen in the spectrum of Figure 19a at *m/z* 178, 228, and 252, respectively, whereas they are not seen in the mass spectrum obtained from blank soil in Figure 19b. Since the organic content of the soil was high, multiple peaks originating from the soil matrix appear in both spectra. PAHs with three or more rings naturally tend to accumulate in the humic fraction of soil [115] with the effect of reducing the desorption efficiency and the S/N values of the analytes in the mass spectrum. Thus, obtaining good results for a soil with high organic content confirms the suitability of the method for the analysis of authentic samples. The concentrations of the compounds spiked to the soil sample (10 µg/g) were in the range observed in areas where anthropogenic pollution occurs [160,161], suggesting that DAPPI-MS would be well suited for the screening analysis of contaminated soils. The sources of PAH contamination in soil samples could perhaps be evaluated on the basis of different compound profiles. In its present form, the method is not suited for the analysis of individual PAHs since the mass peaks of PAHs with the same molecular mass would overlap in the spectra and, judging from the MS/MS experiments, PAHs do not fragment well enough in ion trap MS to produce clear MS/MS spectra.

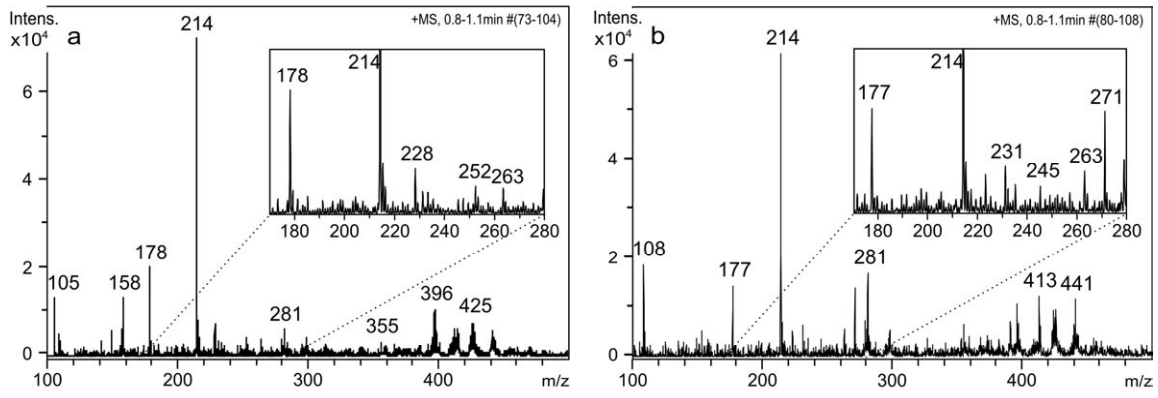

Figure 19 *The DAPPI mass spectrum obtained from (a) spiked soil pellet and (b) blank soil pellet in positive ion mode with toluene (10 µL/min) as the spray solvent. In (a), mass peaks originating from phenantherene, chrysene, and BkF are seen at* m/z *178 ($M^{+\bullet}$),* m/z *228 ($M^{+\bullet}$), and* m/z *252 ($M^{+\bullet}$), respectively. The amount of each PAH compound was 10 µg/g of soil.*

Analysis of drug samples – DAPPI-MS and DESI-MS

The analytical performance of DAPPI-MS with toluene or acetone as spray solvent was compared with that of DESI-MS in the analysis of drug samples 1-9 (Table 12). DESI was included in the study since, on several occasions, it has performed well in drug analysis [76,99,162]. The samples of confiscated drugs that were investigated included powders of amphetamine, cocaine, heroin, methamphetamine, and MDMA. All the powders contained cutting agents (e.g., caffeine and phenacetine). The same powder samples were also identified by GC-MS, and quantified by LC coupled to a UV detector, or by GC coupled to FID, to obtain reference data and the analyte mass percentages (for details see Paper **V**). All active compounds found by GC-MS analysis were also observed in DAPPI-MS and DESI-MS analysis. The compounds were further studied by tandem mass spectrometric (MS/MS) analysis of the radical cations or the protonated molecules.

Basic analytes, such as amphetamine (Samples 1, 2, and 7), MDMA (Sample 2), and methamphetamine (Samples 3 and 9), were observed as $[M+H]^+$ ions with both desorption/ionization methods and both DAPPI spray solvents. This result can be explained by the high PA of these analytes. The DAPPI-MS analyses of heroin (Samples 4 and 8) and cocaine (Samples 5 and 6) gave mostly $M^{+\bullet}$ ions, with a minor proportion of $[M+H]^+$ ions, with toluene as spray solvent, and solely $[M+H]^+$ ions with acetone. It should be noted, however, that the ^{13}C isotope of the $M^{+\bullet}$ ions shares the same *m/z* value as $[M+H]^+$ ions, and the ions at $[M+1]^+$ do not, therefore, solely result from protonation. As an example of the DAPPI-MS and DESI-MS results, MS and MS/MS spectra recorded from Sample 4 (heroin) are presented in Figure 20: the spectra obtained with DAPPI-MS with toluene and acetone as spray solvent in Figure 20a and 20b and the spectrum obtained with DESI-MS in Figure 20c.

Ions from other compounds besides the main active compounds were observed in the spectra. Caffeine was detected in Samples 1 and 2 and phenacetine in Sample 5 by both DAPPI-MS and DESI-MS and also by GC-MS. Caffeine and phenacetine produced $M^{+\bullet}$ ions in DAPPI with toluene as the spray solvent, and $[M+H]^+$ ions in DAPPI with acetone as the spray solvent. The $M^{+\bullet}$ ions of caffeine (*m/z* 194) overlapped with the $[M+H]^+$ ions of MDMA in the MS spectra, but the two species could be distinguished by MS/MS. As can be seen from the spectra in Figure 20, Sample 4 (heroin) gave rise to several mass peaks. The other ions, in addition to those at *m/z* 369 and *m/z* 370 due to heroin, probably originated from some of the common impurities in the drug. Although the impurities were not analyzed thoroughly, the *m/z* values of the most prominent ions [163] suggested the presence of acetylcodeine (*m/z* 341 in Figure 20a, *m/z* 342 in Figure 20b and 20c), papaverine (*m/z* 339 in Figure 20a, *m/z* 340 in Figure 20b and 20c), and monoacetylmorphine (*m/z* 327 in Figure 20a, *m/z* 328 in Figure 20b and 20c). Monoacetylmorphine was also a fragment of heroin in MS/MS analysis, since product ions appeared at *m/z* 327 (Figure 20a) and *m/z* 328 (Figure 20b and 20c) in the MS/MS spectra.

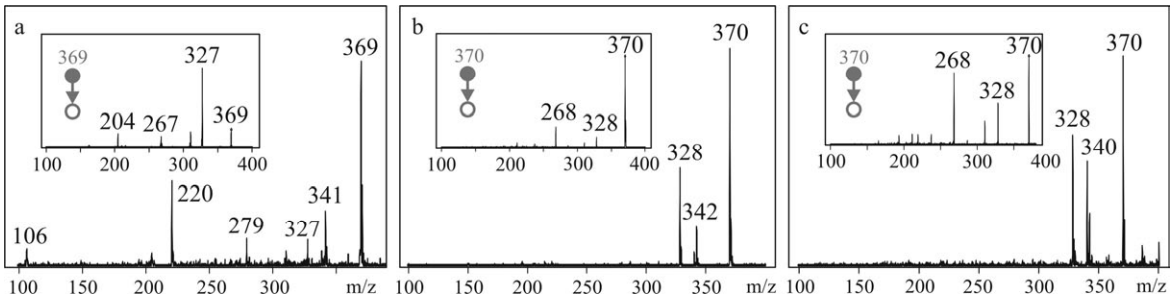

Figure 20 *(a) DAPPI-MS spectrum of Sample 4 obtained with toluene as the spray solvent. Product ion spectrum of m/z 369 ($M^{+\bullet}$ of heroin) is shown in the insert. (b) DAPPI-MS spectrum of Sample 4 obtained with acetone as the spray solvent. Product ion spectrum of m/z 370 ($[M+H]^+$ of heroin) is shown in the insert. (c) DESI-MS spectrum of Sample 4. Product ion spectrum of m/z 370 ($[M+H]^+$ of heroin) is shown in the insert. For details see Paper* ***V****.*

DAPPI-MS and DESI-MS methods are not quantitative, and there were fairly large differences in spot-to-spot signal intensities. Sensitivity comparisons are not reasonable due to the limited data, but also to the nature of the samples. Confiscated drugs typically contain various amounts of cutting agents, which may hinder thermal desorption in DAPPI and droplet pick-up in DESI. The matrix species may also compete with the analytes for the charge and reduce the sensitivity. Therefore, what is true for one sample is not necessarily true for one with a different matrix. Some general trends are nevertheless evident (for details see Table 1 in Paper **V**). Less polar and nonpolar analytes are preferably analyzed by DAPPI-MS with toluene as spray solvent and polar and high-proton affinity compounds by DAPPI-MS with acetone as spray solvent or DESI-MS.

6.2.6 LODs for selected compounds

To evaluate the analytical performance of DAPPI-MS, LODs (S/N ≥ 3) were determined for a set of selected compounds: five PAHs, one N-PAH, one BFR, and nine pesticides (**IV**). The analysis was done in full-scan MS mode with an ion trap MS, and the LODs were determined as average values for four replicate sample spots of standard compounds on a PMMA sampling surface (Table 13). For the PAH compounds the LODs were determined in positive ion mode and they ranged from 0.1 to 1 ng. As expected, LODs were lowest for the largest molecules since the amount of delocalized electrons increases with molecular size, leading to lower IE. Naphthalene, the PAH compound with lowest molecular weight and highest IE (8.144 eV [33]), was not detected at all. Acridine did not follow the pattern, since the nitrogen atom in the structure gives it a significantly higher PA than for the other compounds. The LOD for TBBPA in negative ion mode was 300 pg. The LODs for the pesticides were determined in positive ion mode and ranged from 30 to 300 pg. Values were not significantly different for the different pesticides, evidently because of the similarity of the molecules, i.e., functional groups containing oxygen and nitrogen. LODs in the same range have been reported for pesticides in a previous study by DESI-MS, e.g., 30 pg for imazalil and 150 pg for thiabendazole [93].

Table 13. *Limits of detection (LODs, with S/N≥3), and ions and spray solvents used in the determination of the LODs. Ac stands for acetone, T for toluene and An for anisole.*

Compound	Spray solvent	Ion (m/z)	LOD (pg)	LOD (pmol)
PAHs				
Naphthalene	T	-	-	-
Phenanthrene	T	$M^{+\bullet}$ (178)	1000	5.6
Acridine	Ac	$[M+H]^+$ (180)	100	0.56
Chrysene	T	$M^{+\bullet}$ (228)	300	1.3
BaP	T	$M^{+\bullet}$ (252)	100	0.40
BkF	T	$M^{+\bullet}$ (252)	100	0.40
BFR				
TBBPA	An	$[M-H]^-$ (543)	300	0.55
Pesticides				
Aldicarb	Ac	$[M-CH_3NHCOO]^+$ (116)	100	0.53
Carbofuran	Ac	$[M+H]^+$ (222)	30	0.14
Ditalimfos	Ac	$[M+33]^+$ (332)	100	0.33
Imazalil	Ac	$[M+H]^+$ (297)	100	0.34
Methiocarb	Ac	$[M+H]^+$ (226)	100	0.44
Methomyl	Ac	$[M+H]^+$ (163)	100	0.62
Oxamyl	Ac	$[M+H-(CH_3)_2NCO-CH_3NHCO]^+$ (90)	300	1.4
Pirimicarb	Ac	$[M+H]^+$ (239)	100	0.42
Thiabendazole	Ac	$[M+H]^+$ (202)	100	0.50

Abbreviations for analytes in Table 13:

BaP	Benzo[a]pyrene
BkF	Benzo[k]fluoranthene
TBBPA	Tetrabromobisphenol A

7 Summary and conclusions

Novel atmospheric pressure ionization techniques based on APCI and APPI were studied and evaluated in environmental analysis and bioanalysis. The techniques were used in GC-µAPCI-MS, GC-µAPPI-MS, and DAPPI-MS instrumentations. Miniaturized APCI and APPI ion sources are rare, which makes the GC-µAPCI-MS and GC-µAPPI-MS instrumentations and the presented methods exceptional. The studies of DAPPI are unique since DAPPI was developed in our research group and is not applied elsewhere.

The API microchips, the basic hardware for the µAPCI, µAPPI and DAPPI techniques, were manufactured by microfabrication methods allowing their mass production. The manufacturing costs for a single API microchip are thus a fraction of those for conventional, normal-scale ion sources. In addition, the API microchips are durable, and a single microchip can be used for weeks without malfunction. µAPCI and µAPPI can be used in coupling of a gas chromatograph to any mass spectrometer with API interface.

The feasibility of the GC-µAPCI-MS and GC-µAPPI-MS techniques was demonstrated in environmental analysis of PCBs and in bioanalysis of 2-quinolinone-derived SARMs. In negative ion mode, the analytical characteristics (LODs, linear ranges, and intra-day repeatabilities) of GC-µAPCI-MS and GC-µAPPI-MS were studied with PCB standards and confirmed to be good. In addition, the analysis of authentic environmental samples for PCBs by GC-µAPPI-MS showed the potential of the technique for quantitative analysis. The quantitation results obtained with GC-µAPPI-MS were consistent with results obtained with the established analytical technique, GC-ECD. However, the sensitivity of GC-µAPPI-MS with an ion trap MS was probably lower than that of GC-ECD, which is highly sensitive for the analysis of PCBs. In positive ion mode, the analytical characteristics of GC-µAPPI-MS were studied with novel potential doping compounds, 2-quinolinone-derived SARMs in spiked urine samples. Excellent analytical characteristics were demonstrated. Sensitivity of the GC-µAPPI-MS method was similar to that of reported analytical methods for 2-quinolinone-derived SARMs (LC-ESI-MS and GC-EI-MS). In addition, the possibility to combine the API microchip with a high-resolution MS instrument (GC-µAPCI-Orbitrap MS) was demonstrated.

Although GC-µAPCI-MS and GC-µAPPI-MS techniques offered high analytical performance (low LODs, wide linear ranges, and good repeatabilities), further optimization of the ion source is needed to enhance the usability of the devices. Assembling of µAPCI and µAPPI devices is a challenging task for to two reasons. First, the space in front of the MS inlet is limited, and accommodation of all the parts needed for operating the µAPCI or µAPPI is challenging. Second, the sample plume produced by the API microchip is narrow (cross-section ~ 1 mm) and positioning of the API microchip in relation to the MS inlet requires fine tuning. The corona discharge needle (µAPCI) and the UV lamp (µAPPI) also need to be positioned carefully to avoid repeatability problems. In addition, in the open ion source design the repeatability of the ionization process may be compromised by gases and particles in the laboratory air entering the ionization area. The above mentioned issues complicate the use of instrumentation, although high quality analyses are still achievable. These challenges could be overcome by a stable custom-made ion source platform including a holder for the API microchip and corona discharge needle or UV lamp, integrated heating power and auxiliary gas connections, and a shielding case over the entire ion source. The introduction of an ion source platform would

enable more accurate positioning of the ion source parts and a more stable ionization environment, and thus more repeatable and sensitive analytics.

The DAPPI-MS technique employs thermal desorption and subsequent photoionization of analytes from surfaces and can be used for direct analysis of solid samples. Solid sample surfaces, such as plants and compressed soil, can be analyzed directly, without prior sample treatment. Analysis of dried sample droplets on a surface is also possible. Because there is no sample pretreatment step, the DAPPI-MS method is faster than the conventional infusion methods involving APPI-MS. In addition, DAPPI-MS is a feasible and sensitive technique for the analysis of very small sample volumes. In comparison with the most popular ambient desorption/ionization technique, DESI, DAPPI performs well in the analysis of nonpolar compounds, which are not amenable to normal DESI.

Desorption in DAPPI was found to be a thermal process, whose efficiency is largely determined by the thermal conductivity of the sampling surface. The ionization takes place in gas phase through similar reactions to those APPI. The ionization mechanism is determined by IE and PA of the spray solvent and the analyte in positive ion mode, and by the EA and gas-phase acidity of the spray solvent and the analyte in negative ion mode. DAPPI-MS was utilized in fast screening for PAHs, BFR, pesticides, and illicit drugs in authentic samples (circuit board, orange peel, and confiscated drug powders) and in a spiked soil sample. These applications in environmental, food, and forensic analysis demonstrated the feasibility of DAPPI-MS for rapid screening of authentic samples.

The drawback of fast and direct sampling in DAPPI-MS is the contamination of the MS ion optics since, in addition to the target analytes in the sample, the heated vapor plume may desorb large amounts of other compounds able to contaminate the MS and increase background noise. Contamination leads to decreased sensitivity of the analysis, and thus decreased reliability. This is not solely a problem to DAPPI, however, but for many other ambient desorption/ionization techniques as well.

In summary, the methods presented in this thesis show the applicability of the recently developed API microchips in real-life analytical work, and versatility of the API microchips for different modes. µAPCI and µAPPI enable the coupling of gas chromatographs to any mass spectrometer with API interface, and GC-µAPCI-MS and GC-µAPPI-MS methods have potential for quantitative analysis. DAPPI is an efficient ambient desorption/ionization technique for solid samples, and for a wide range of analytes of different polarities, including neutral and completely nonpolar compounds. DAPPI-MS is suitable for qualitative rapid screening analysis.

References

1. Erickson, D.; Li, D. Integrated microfluidic devices. *Anal. Chim. Acta.* **2004**, *507*, 11-26.
2. Foret, F.; Kusy, P. Microdevices in mass spectrometry. *Eur. J. Mass Spectrom.* **2007**, *13*, 41-44.
3. Koster, S.; Verpoorte, E. A decade of microfluidic analysis coupled with electrospray mass spectrometry: An overview. *Lab Chip.* **2007**, *7*, 1394-1412.
4. Sikanen, T.; Franssila, S.; Kauppila, T. J.; Kostiainen, R.; Kotiaho, T.; Ketola, R. A. Microchip technology in mass spectrometry. *Mass Spectrom. Rev.* **2010**.
5. Venter, A.; Nefliu, M.; Cooks, R. G. Ambient desorption ionization mass spectrometry. *TrAC.* **2008**, *27*, 284-290.
6. Van Berkel, G. J.; Pasilis, S. P.; Ovchinnikova, O. Established and emerging atmospheric pressure surface sampling/ionization techniques for mass spectrometry. *J. Mass Spectrom.* **2008**, *43*, 1161-1180.
7. Takats, Z.; Wiseman, J. M.; Gologan, B.; Cooks, R. G. Mass spectrometry sampling under ambient conditions with desorption electrospray ionization. *Science.* **2004**, *306*, 471-473.
8. Haapala, M.; Pól, J.; Saarela, V.; Arvola, V.; Kotiaho, T.; Ketola, R. A.; Franssila, S.; Kauppila, T. J.; Kostiainen, R. Desorption atmospheric pressure photoionization. *Anal. Chem.* **2007**, *79*, 7867-7872.
9. Manahan, S. E. Environmental chemistry, 9th ed.; CRC Press, Boca Raton, Florida, 2000.
10. Beyer, A.; Biziuk, M. Environmental fate and global distribution of polychlorinated biphenyls. *Rev. Environ. Contam. Toxicol.* **2009**, *201*, 137-158.
11. Deroo, B. J.; Burns, K. A.; Winuthayanon, W.; Korach, K. S. Potential effects for environmental xeno-estrogens pollution and fertility. *Biochemist.* **2009**, *31*, 2.
12. Calisto, V.; Esteves, V. I. Psychiatric pharmaceuticals in the environment. *Chemosphere.* **2009**, *77*, 1257-1274.
13. Buchanan, I.; Liang, H. C.; Khan, W.; Liu, Z.; Singh, R.; Ikehata, K.; Chelme-Ayala, P. Pesticides and herbicides [in the environment]. *Water Environ Res.* **2009**, *81*, 1731-1316.
14. Isaacson, C. W.; Kleber, M.; Field, J. A. Quantitative analysis of fullerene nanomaterials in environmental systems: A critical review. *Environ. Sci. Technol.* **2009**, *43*, 6463-6474.
15. Soldin, S. J.; Soldin, O. P. Steroid hormone analysis by tandem mass spectrometry. *Clin. Chem.* **2009**, *55*, 1061-1066.
16. Thevis, M.; Thomas, A.; Kohler, M.; Beuck, S.; Schanzer, W. Emerging drugs: Mechanism of action, mass spectrometry and doping control analysis. *J. Mass Spectrom.* **2009**, *44*, 442-460.
17. Ma, S.; Zhu, M. Recent advances in applications of liquid chromatography-tandem mass spectrometry to the analysis of reactive drug metabolites. *Chem. Biol. Interact.* **2009**, *179*, 25-37.
18. Rubio, S.; Perez-Bendito, D. Recent advances in environmental analysis. *Anal. Chem.* **2009**, *81*, 4601-4622.
19. Covey, T. R.; Thomson, B. A.; Schneider, B. B. Atmospheric pressure ion sources. *Mass Spectrom. Rev.* **2009**, *28*, 870-897.
20. Dole, M.; Mack, L. L.; Hines, R. L. Molecular beams of macroions. *J. Chem. Phys.* **1968**, *49*, 2240.

21. Yamashita, M.; Fenn, J. B. Electrospray ion source. Another variation on the free-jet theme. *J. Phys. Chem.* **1984**, *88*, 4451-4459.
22. Bruins, A. P.; Covey, T. R.; Henion, J. D. Ion spray interface for combined liquid chromatography/atmospheric pressure ionization mass spectrometry. *Anal. Chem.* **1987**, *59*, 2642-2646.
23. Horning, E. C.; Horning, M. G.; Carroll, D. I.; Dzidic, I.; Stillwell, R. N. New picogram detection system based on a mass spetrometer with an ionization source at atmospheric pressure. *Anal. Chem.* **1973**, *45*, 936-943.
24. Carroll, D. I.; Dzidic, I.; Stillwell, R. N.; Haegele, K. D.; Horning, E. C. Atmospheric pressure ionization mass spectrometry. Corona discharge ion source in liquid chromatograph-mass spectrometer-computer analytical system. *Anal. Chem.* **1975**, *47*, 2369-2373.
25. Robb, D. B.; Covey, T. R.; Bruins, A. P. Atmospheric pressure photoionization: An ionization method for liquid chromatography-mass spectrometry. *Anal. Chem.* **2000**, *72*, 3653-3659.
26. Syage, J. A.; Evans, M. D. Photoionization mass spectrometry – A powerful new tool for drug discovery. *Spectroscopy*. **2001**, *16*, 14-21.
27. Gross, J. H. Electrospray ionization. In *Mass Spectrometry: A Textbook*, 1st ed.; Gross, J. H., Ed.; Springer, Berlin. Germany, 2004; p. 441.
28. Fenn, J. B.; Mann, M.; Meng, C. K.; Wong, S. F.; Whitehouse, C. M. Electrospray ionization for mass spectrometry of large biomolecules. *Science*. **1989**, *246*, 64-71.
29. Niessen, W. M. A. Liquid chromatography-mass spectrometry, 3rd ed.; CRC Press Taylor & Francis Group, Boca Raton, Florida, 2006.
30. Carroll, D. I.; Dzidic, I.; Horning, E. C.; Stillwell, R. N. Atmospheric-pressure ionization mass spectrometry. *Appl. Spectrosc. Rev.* **1981**, *17*, 337-406.
31. Dzidic, I.; Carroll, D. I.; Stillwell, R. N.; Horning, E. C. Gas phase reactions. Ionization by proton transfer to superoxide anions. *J. Am. Chem. Soc.* **1974**, *96*, 5258-5259.
32. Dzidic, I.; Carroll, D. I.; Stillwell, R. N.; Horning, E. C. Atmospheric pressure ionization (API) mass spectrometry: Formation of phenoxide ions from chlorinated aromatic compounds. *Anal. Chem.* **1975**, *47*, 1308-1312.
33. "Gas phase ion energetics data" in NIST Chemistry WebBook, NIST Standard reference database Number 69, June 2005. http://webbook.nist.gov
34. Horning, E. C.; Carroll, D. I.; Dzidic, I.; Lin, S.-N.; Stillwell, R. N.; Thenot, J.-P. Atmospheric pressure ionization mass spectrometry. Studies of negative ion formation for detection and quantification purposes. *J. Chromatogr.* **1977**, *142*, 481-495.
35. Debrauwer, L.; Riu, A.; Jouahri, M.; Rathahao, E.; Jouanin, I.; Antignac, J. P.; Cariou, R.; Le Bize, B.; Zalko, D. Probing new approaches using atmospheric pressure photo ionization for the analysis of brominated flame retardants and their related degradation products by liquid chromatography-mass spectrometry. *J. Chromatogr. A.* **2005**, *1082*, 98-109.
36. Kauppila, T. J.; Kotiaho, T.; Bruins, A. P.; Kostiainen, R. Negative ion-atmospheric pressure photoionization-mass spectrometry. *J. Am. Soc. Mass Spectrom.* **2004**, *15*, 203-211.
37. McEwen, C. N.; McKay, R. G. A combination atmospheric pressure LC/MS:GC/MS ion source: Advantages of dual AP-LC/MS:GC/MS instrumentation. *J. Am. Soc. Mass Spectrom.* **2005**, *16*, 1730-1738.
38. Schiewek, R.; Lorenz, M.; Giese, R.; Brockmann, K.; Benter, T.; Gab, S.; Schmitz, O. J. Development of a multipurpose ion source for LC-MS and GC-API MS. *Anal. Bioanal. Chem.* **2008**, *392*, 87-96.

39. Hanold, K. A.; Fischer, S. M.; Cormia, P. H.; Miller, C. E.; Syage, J. A. Atmospheric pressure photoionization. 1. General properties for LC/MS. *Anal. Chem.* **2004**, *76*, 2842-2851.
40. Kauppila, T. J.; Kuuranne, T.; Meurer, E. C.; Eberlin, M. N.; Kotiaho, T.; Kostiainen, R. Atmospheric pressure photoionization mass spectrometry. Ionization mechanism and the effect of solvent on the ionization of naphthalenes. *Anal. Chem.* **2002**, *74*, 5470-5479.
41. Munson, M. S. B. Reaction of gaseous bronsted acids. *J. Am. Chem. Soc.* **1965**, *87*, 5313-5317.
42. Tzeng, W. B.; Wei, S.; Castleman, A. W., Jr. Multiphoton ionization of acetone clusters: Metastable unimolecular decomposition of acetone cluster ions and the influence of solvation on intracluster ion-molecule reactions. *J. Am. Chem. Soc.* **1989**, *111*, 6035-6040.
43. Basso, E.; Marotta, E.; Seraglia, R.; Tubaro, M.; Traldi, P. On the formation of negative ions in atmospheric pressure photoionization conditions. *J. Mass Spectrom.* **2003**, *38*, 1113-1115.
44. Marchi, I.; Rudaz, S.; Veuthey, J. L. Atmospheric pressure photoionization for coupling liquid-chromatography to mass spectrometry: A review. *Talanta.* **2009**, *78*, 1-18.
45. McEwen, C. N. GC/MS on an LC/MS instrument using atmospheric pressure photoionization. *Int. J. Mass Spectrom.* **2007**, *259*, 57-64.
46. Revelsky, I. A.; Yashin, Y. S.; Sobolevsky, T. G.; Revelsky, A. I.; Miller, B.; Oriedo, V. Electron ionization and atmospheric pressure photochemical ionization in gas chromatography-mass spectrometry analysis of amino acids. *Eur. J. Mass. Spectrom.* **2003**, *9*, 497-507.
47. Wood, T. D.; Moy, M. S.; Dolan, A. R.; Bigwarfe, P. M.,Jr.; White, T. P.; Smith, D. R.; Higbee, D. J. Miniaturization of electrospray ionization mass spectrometry. *Appl. Spectrosc. Rev.* **2003**, *38*, 187-244.
48. Östman, P.; Marttila, S. J.; Kotiaho, T.; Franssila, S.; Kostiainen, R. Microchip atmospheric pressure chemical ionization source for mass spectrometry. *Anal. Chem.* **2004**, *76*, 6659-6664.
49. Kauppila, T. J.; Östman, P.; Marttila, S.; Ketola, R. A.; Kotiaho, T.; Franssila, S.; Kostiainen, R. Atmospheric pressure photoionization-mass spectrometry with a microchip heated nebulizer. *Anal. Chem.* **2004**, *76*, 6797-6801.
50. Pól, J.; Kauppila, T. J.; Haapala, M.; Saarela, V.; Franssila, S.; Ketola, R. A.; Kotiaho, T.; Kostiainen, R. Microchip sonic spray ionization. *Anal. Chem.* **2007**, *79*, 3519-3523.
51. Keski-Rahkonen, P.; Haapala, M.; Saarela, V.; Franssila, S.; Kotiaho, T.; Kostiainen, R.; Auriola, S. Atmospheric pressure thermospray ionization using a heated microchip nebulizer. *Rapid Commun. Mass Spectrom.* **2009**, *23*, 3313-3322.
52. Pól, J.; Kauppila, T. J.; Franssila, S.; Kotiaho, T.; Kostiainen, R. Ionspray microchip. *Rapid Commun. Mass Spectrom.* **2010**, *submitted.*
53. Östman, P.; Jäntti, S.; Grigoras, K.; Saarela, V.; Ketola, R. A.; Franssila, S.; Kotiaho, T.; Kostiainen, R. Capillary liquid chromatography-microchip atmospheric pressure chemical ionization-mass spectrometry. *Lab Chip.* **2006**, *6*, 948-953.
54. Haapala, M.; Luosujärvi, L.; Saarela, V.; Kotiaho, T.; Ketola, R. A.; Franssila, S.; Kostiainen, R. Microchip for combining gas chromatography or capillary liquid chromatography with atmospheric pressure photoionization-mass spectrometry. *Anal. Chem.* **2007**, *79*, 4994-4999.

55. Östman, P.; Luosujärvi, L.; Haapala, M.; Grigoras, K.; Ketola, R. A.; Kotiaho, T.; Franssila, S.; Kostiainen, R. Gas chromatography-microchip atmospheric pressure chemical ionization-mass spectrometry. *Anal. Chem.* **2006**, *78*, 3027-3031.
56. Ahonen, L. L.; Haapala, M.; Saarela, V.; Franssila, S.; Kotiaho, T.; Kostiainen, R. Feasibility of capillary liquid chromatography/microchip atmospheric pressure photoionization mass spectrometry in analyzing anabolic steroids in urine samples. *Rapid Commun. Mass Spectrom.* **2010**, *24*, 958-964.
57. Cody, R. B.; Laramee, J. A.; Durst, H. D. Versatile new ion source for the analysis of materials in open air under ambient conditions. *Anal. Chem.* **2005**, *77*, 2297-2302.
58. Chen, H.; Gamez, G.; Zenobi, R. What can we learn from ambient ionization techniques? *J. Am. Soc. Mass Spectrom.* **2009**, *20*, 1947-1963.
59. Weston, D. J. Ambient ionization mass spectrometry: Current understanding of mechanistic theory; analytical performance and application areas. *Analyst.* **2010**, *135*, 661-668.
60. Chen, H.; Ouyang, Z.; Cooks, R. G. Thermal production and reactions of organic ions at atmospheric pressure. *Angew. Chem.* **2006**, *45*, 3656-3660.
61. Ebejer, K. A.; Brereton, R. G.; Carter, J. F.; Ollerton, S. L.; Sleeman, R. Rapid comparison of diacetylmorphine on banknotes by tandem mass spectrometry. *Rapid Commun. Mass Spectrom.* **2005**, *19*, 2137-2143.
62. McEwen, C. N.; McKay, R. G.; Larsen, B. S. Analysis of solids, liquids, and biological tissues using solids probe introduction at atmospheric pressure on commercial LC/MS instruments. *Anal. Chem.* **2005**, *77*, 7826-7831.
63. Wu, J.; Hughes, C. S.; Picard, P.; Letarte, S.; Gaudreault, M.; Levesque, J. F.; Nicoll-Griffith, D. A.; Bateman, K. P. High-throughput cytochrome P450 inhibition assays using laser diode thermal desorption-atmospheric pressure chemical ionization-tandem mass spectrometry. *Anal. Chem.* **2007**, *79*, 4657-4665.
64. Williams, J. P.; Scrivens, J. H. Rapid accurate mass desorption electrospray ionisation tandem mass spectrometry of pharmaceutical samples. *Rapid Commun. Mass Spectrom.* **2005**, *19*, 3643-3650.
65. Ratcliffe, L. V.; Rutten, F. J.; Barrett, D. A.; Whitmore, T.; Seymour, D.; Greenwood, C.; Aranda-Gonzalvo, Y.; Robinson, S.; McCoustra, M. Surface analysis under ambient conditions using plasma-assisted desorption/ionization mass spectrometry. *Anal. Chem.* **2007**, *79*, 6094-6101.
66. Na, N.; Zhao, M.; Zhang, S.; Yang, C.; Zhang, X. Development of a dielectric barrier discharge ion source for ambient mass spectrometry. *J. Am. Soc. Mass Spectrom.* **2007**, *18*, 1859-1862.
67. Andrade, F. J.; Shelley, J. T.; Wetzel, W. C.; Webb, M. R.; Gamez, G.; Ray, S. J.; Hieftje, G. M. Atmospheric pressure chemical ionization source. 2. Desorption-ionization for the direct analysis of solid compounds. *Anal. Chem.* **2008**, *80*, 2654-2663.
68. Günther, D.; Hattendorf, B. Solid sample analysis using laser ablation inductively coupled plasma mass spectrometry. *TrAC.* **2005**, *24*, 255-265.
69. Mokgalaka, N.; Gardea-Torresdey, J. L. Laser ablation inductively coupled plasma mass spectrometry: Principles and applications. *Appl. Spectrosc. Rev.* **2006**, *41*, 131-150.
70. Coon, J. J.; McHale, K. J.; Harrison, W. W. Atmospheric pressure laser desorption/chemical ionization mass spectrometry: A new ionization method based on existing themes. *Rapid Commun. Mass Spectrom.* **2002**, *16*, 681-685.
71. Shiea, J.; Huang, M. Z.; Hsu, H. J.; Lee, C. Y.; Yuan, C. H.; Beech, I.; Sunner, J. Electrospray-assisted laser desorption/ionization mass spectrometry for direct ambient analysis of solids. *Rapid Commun. Mass Spectrom.* **2005**, *19*, 3701-3704.

72. Nemes, P.; Vertes, A. Laser ablation electrospray ionization for atmospheric pressure, *in vivo*, and imaging mass spectrometry. *Anal. Chem.* **2007**, *79*, 8098-8106.
73. Rezenom, Y. H.; Dong, J.; Murray, K. K. Infrared laser-assisted desorption electrospray ionization mass spectrometry. *Analyst.* **2008**, *133*, 226-232.
74. Cooks, R. G.; Ouyang, Z.; Takats, Z.; Wiseman, J. M. Detection technologies. Ambient mass spectrometry. *Science.* **2006**, *311*, 1566-1570.
75. Haddad, R.; Sparrapan, R.; Eberlin, M. N. Desorption sonic spray ionization for (high) voltage-free ambient mass spectrometry. *Rapid Commun. Mass Spectrom.* **2006**, *20*, 2901-2905.
76. Haddad, R.; Sparrapan, R.; Kotiaho, T.; Eberlin, M. N. Easy ambient sonic-spray ionization-membrane interface mass spectrometry for direct analysis of solution constituents. *Anal. Chem.* **2008**, *80*, 898-903.
77. Haddad, R.; Milagre, H. M.; Catharino, R. R.; Eberlin, M. N. Easy ambient sonic-spray ionization mass spectrometry combined with thin-layer chromatography. *Anal. Chem.* **2008**, *80*, 2744-2750.
78. Chen, H.; Wortmann, A.; Zenobi, R. Neutral desorption sampling coupled to extractive electrospray ionization mass spectrometry for rapid differentiation of biosamples by metabolomic fingerprinting. *J. Mass Spectrom.* **2007**, *42*, 1123-1135.
79. Van Berkel, G. J.; Ford, M. J.; Doktycz, M. J.; Kennel, S. J. Evaluation of a surface-sampling probe electrospray mass spectrometry system for the analysis of surface-deposited and affinity-captured proteins. *Rapid Commun. Mass Spectrom.* **2006**, *20*, 1144-1152.
80. Luftmann, H. A simple device for the extraction of TLC spots: Direct coupling with an electrospray mass spectrometer. *Anal. Bioanal. Chem.* **2004**, *378*, 964-968.
81. Takats, Z.; Wiseman, J. M.; Cooks, R. G. Ambient mass spectrometry using desorption electrospray ionization (DESI): Instrumentation, mechanisms and applications in forensics, chemistry, and biology. *J. Mass Spectrom.* **2005**, *40*, 1261-1275.
82. Wu, C.; Ifa, D. R.; Manicke, N. E.; Cooks, R. G. Molecular imaging of adrenal gland by desorption electrospray ionization mass spectrometry. *Analyst.* **2010**, *135*, 28-32.
83. Wu, C.; Qian, K.; Nefliu, M.; Cooks, R. G. Ambient analysis of saturated hydrocarbons using discharge-induced oxidation in desorption electrospray ionization. *J. Am. Soc. Mass Spectrom.* **2010**, *21*, 261-267.
84. Mulligan, C. C.; MacMillan, D. K.; Noll, R. J.; Cooks, R. G. Fast analysis of high-energy compounds and agricultural chemicals in water with desorption electrospray ionization mass spectrometry. *Rapid Commun. Mass Spectrom.* **2007**, *21*, 3729-3736.
85. Pól, J.; Vidová, V.; Kruppa, G.; Kobliha, V.; Novák, P.; Lemr, K.; Kotiaho, T.; Kostiainen, R.; Havlíček, V.; Volný, M. Automated ambient desorption-ionization platform for surface imaging integrated with a commercial fourier transform ion cyclotron resonance mass spectrometer. *Anal. Chem.* **2009**, *81*, 8479-8487.
86. Lane, A. L.; Nyadong, L.; Galhena, A. S.; Shearer, T. L.; Stout, E. P.; Parry, R. M.; Kwasnik, M.; Wang, M. D.; Hay, M. E.; Fernandez, F. M.; Kubanek, J. Desorption electrospray ionization mass spectrometry reveals surface-mediated antifungal chemical defense of a tropical seaweed. *Proc. Natl. Acad. Sci. U.S.A.* **2009**, *106*, 7314-7319.
87. Nyadong, L.; Hohenstein, E. G.; Galhena, A.; Lane, A. L.; Kubanek, J.; Sherrill, C. D.; Fernandez, F. M. Reactive desorption electrospray ionization mass spectrometry (DESI-MS) of natural products of a marine alga. *Anal. Bioanal. Chem.* **2009**, *394*, 245-254.

88. Jackson, A. U.; Tata, A.; Wu, C.; Perry, R. H.; Haas, G.; West, L.; Cooks, R. G. Direct analysis of stevia leaves for diterpene glycosides by desorption electrospray ionization mass spectrometry. *Analyst.* **2009**, *134*, 867-874.
89. Dill, A. L.; Ifa, D. R.; Manicke, N. E.; Costa, A. B.; Ramos-Vara, J. A.; Knapp, D. W.; Cooks, R. G. Lipid profiles of canine invasive transitional cell carcinoma of the urinary bladder and adjacent normal tissue by desorption electrospray ionization imaging mass spectrometry. *Anal. Chem.* **2009**, *81*, 8758-8764.
90. Wu, C.; Ifa, D. R.; Manicke, N. E.; Cooks, R. G. Rapid, direct analysis of cholesterol by charge labeling in reactive desorption electrospray ionization. *Anal. Chem.* **2009**, *81*, 7618-7624.
91. Dill, A. L.; Ifa, D. R.; Manicke, N. E.; Ouyang, Z.; Cooks, R. G. Mass spectrometric imaging of lipids using desorption electrospray ionization. *J. Chromatogr. B.* **2009**, *877*, 2883-2889.
92. Manicke, N. E.; Wiseman, J. M.; Ifa, D. R.; Cooks, R. G. Desorption electrospray ionization (DESI) mass spectrometry and tandem mass spectrometry (MS/MS) of phospholipids and sphingolipids: Ionization, adduct formation, and fragmentation. *J. Am. Soc. Mass Spectrom.* **2008**, *19*, 531-543.
93. Garcia-Reyes, J. F.; Jackson, A. U.; Molina-Diaz, A.; Cooks, R. G. Desorption electrospray ionization mass spectrometry for trace analysis of agrochemicals in food. *Anal. Chem.* **2009**, *81*, 820-829.
94. Kauppila, T. J.; Arvola, V.; Haapala, M.; Pól, J.; Aalberg, L.; Saarela, V.; Franssila, S.; Kotiaho, T.; Kostiainen, R. Direct analysis of illicit drugs by desorption atmospheric pressure photoionization. *Rapid Commun. Mass Spectrom.* **2008**, *22*, 979-985.
95. Rodriguez-Cruz, S. E. Rapid analysis of controlled substances using desorption electrospray ionization mass spectrometry. *Rapid Commun. Mass Spectrom.* **2006**, *20*, 53-60.
96. Leuthold, L. A.; Mandscheff, J. F.; Fathi, M.; Giroud, C.; Augsburger, M.; Varesio, E.; Hopfgartner, G. Desorption electrospray ionization mass spectrometry: Direct toxicological screening and analysis of illicit ecstasy tablets. *Rapid Commun. Mass Spectrom.* **2006**, *20*, 103-110.
97. Kertesz, V.; Van Berkel, G. J.; Vavrek, M.; Koeplinger, K. A.; Schneider, B. B.; Covey, T. R. Comparison of drug distribution images from whole-body thin tissue sections obtained using desorption electrospray ionization tandem mass spectrometry and autoradiography. *Anal. Chem.* **2008**, *80*, 5168-5177.
98. Wiseman, J. M.; Ifa, D. R.; Zhu, Y.; Kissinger, C. B.; Manicke, N. E.; Kissinger, P. T.; Cooks, R. G. Desorption electrospray ionization mass spectrometry: Imaging drugs and metabolites in tissues. *Proc. Natl. Acad. Sci. U.S.A.* **2008**, *105*, 18120-18125.
99. Kauppila, T. J.; Talaty, N.; Kuuranne, T.; Kotiaho, T.; Kostiainen, R.; Cooks, R. G. Rapid analysis of metabolites and drugs of abuse from urine samples by desorption electrospray ionization-mass spectrometry. *Analyst.* **2007**, *132*, 868-875.
100. Haddad, R.; Catharino, R. R.; Marques, L. A.; Eberlin, M. N. Perfume fingerprinting by easy ambient sonic-spray ionization mass spectrometry: Nearly instantaneous typification and counterfeit detection. *Rapid Commun. Mass Spectrom.* **2008**, *22*, 3662-3666.
101. Saunders, K. C.; Ghanem, A.; Boon Hon, W.; Hilder, E. F.; Haddad, P. R. Separation and sample pre-treatment in bioanalysis using monolithic phases: A review. *Anal. Chim. Acta.* **2009**, *652*, 22-31.
102. Ezan, E.; Dubois, M.; Becher, F. Bioanalysis of recombinant proteins and antibodies by mass spectrometry. *Analyst.* **2009**, *134*, 825-834.

103. Marshall, A. G.; Hendrickson, C. L. High-resolution mass spectrometers. *Annu. Rev. Anal. Chem.* **2008**, *1*, 579-599.
104. Facchetti, S. Mass spectrometry in the analysis for polychlorinated biphenyls. *Mass Spectrom. Rev.* **1993**, *12*, 173-203.
105. Poster, D. L.; Schantz, M. M.; Sander, L. C.; Wise, S. A. Analysis of polycyclic aromatic hydrocarbons (PAHs) in environmental samples: A critical review of gas chromatographic (GC) methods. *Anal. Bioanal. Chem.* **2006**, *386*, 859-881.
106. Kierkegaard, A.; Sellstrom, U.; McLachlan, M. S. Environmental analysis of higher brominated diphenyl ethers and decabromodiphenyl ethane. *J. Chromatogr. A.* **2009**, *1216*, 364-375.
107. Dömötörová, M.; Matisová, E. Fast gas chromatography for pesticide residues analysis. *J. Chromatogr. A.* **2008**, *1207*, 1-16.
108. Moriwaki, H. Liquid chromatographic-mass spectrometric methods for the analysis of persistent pollutants: polycyclic aromatic hydrocarbons, organochlorine compounds, and perfluorinated compounds. *Curr. Org. Chem.* **2005**, *9*, 849-957.
109. Covaci, A.; Voorspoels, S.; Abdallah, M. A.; Geens, T.; Harrad, S.; Law, R. J. Analytical and environmental aspects of the flame retardant tetrabromobisphenol-A and its derivatives. *J. Chromatogr. A.* **2009**, *1216*, 346-363.
110. Kuster, M.; Lopez de Alda, M.; Barcelo, D. Liquid chromatography-tandem mass spectrometric analysis and regulatory issues of polar pesticides in natural and treated waters. *J. Chromatogr. A.* **2009**, *1216*, 520-529.
111. Nunez, O.; Moyano, E.; Galceran, M. T. LC-MS/MS analysis of organic toxics in food. *TrAC.* **2005**, *24*, 683-703.
112. Pawliszyn, J. Sampling and sample preparation in field and laboratory, 1st ed.; Elsevier Science, Amsterdam, The Netherlands, 2002.
113. Khan, Z.; Troquet, J.; Vachelard, C. Sample preparation and analytical techniques for determination polyaromatic hydrocarbons in soils. *Int. J. Environ. Sci. Technol.* **2005**, *2*, 275-286.
114. Wilcke, W. Polycyclic aromatic hydrocarbons (PAHs) in soil – A review. *J. Plant Nutr. Soil Sci.* **2000**, *163*, 229-248.
115. Srogi, K. Monitoring of environmental exposure to polycyclic aromatic hydrocarbons: A review. *Environ. Chem. Lett.* **2007**, *5*, 169-195.
116. Hale, R. C.; La Guardia, M. J.; Harvey, E.; Gaylor, M. O.; Mainor, T. M. Brominated flame retardant concentrations and trends in abiotic media. *Chemosphere.* **2006**, *64*, 181-186.
117. Garcia-Jares, C.; Regueiro, J.; Barro, R.; Dagnac, T.; Llompart, M. Analysis of industrial contaminants in indoor air. Part 2. Emergent contaminants and pesticides. *J. Chromatogr. A.* **2009**, *1216*, 567-597.
118. Barro, R.; Regueiro, J.; Llompart, M.; Garcia-Jares, C. Analysis of industrial contaminants in indoor air: Part 1. Volatile organic compounds, carbonyl compounds, polycyclic aromatic hydrocarbons and polychlorinated biphenyls. *J. Chromatogr. A.* **2009**, *1216*, 540-566.
119. Ahmed, F. E. Analysis of polychlorinated biphenyls in food products. *TrAC.* **2003**, *22*, 170-185.
120. Beyer, A.; Biziuk, M. Methods for determining pesticides and polychlorinated biphenyls in food samples – Problems and challenges. *Crit. Rev. Food Sci. Nutr.* **2008**, *48*, 888-904.
121. Thevis, M.; Kohler, M.; Maurer, J.; Schlorer, N.; Kamber, M.; Schanzer, W. Screening for 2-quinolinone-derived selective androgen receptor agonists in doping control analysis. *Rapid Commun. Mass Spectrom.* **2007**, *21*, 3477-3486.
122. Thevis, M.; Kohler, M.; Schlorer, N.; Fussholler, G.; Schanzer, W. Screening for two selective androgen receptor modulators using gas chromatography-mass

spectrometry in doping control analysis. *Eur. J. Mass. Spectrom.* **2008**, *14*, 153-161.

123. Thevis, M.; Schanzer, W. Mass spectrometry of selective androgen receptor modulators. *J. Mass Spectrom.* **2008**, *43*, 865-876.
124. Waddell-Smith, R. J. A review of recent advances in impurity profiling of illicit MDMA samples. *J. Forensic Sci.* **2007**, *52*, 1297-1304.
125. Dams, R.; Benijts, T.; Lambert, W. E.; Massart, D. L.; De Leenheer, A. P. Heroin impurity profiling: Trends throughout a decade of experimenting. *Forensic Sci. Int.* **2001**, *123*, 81-88.
126. Chiarotti, M.; Fucci, N. Comparative analysis of heroin and cocaine seizures. *J. Chromatogr. B.* **1999**, *733*, 127-136.
127. Sleeman, R.; Burton, F.; Carter, J.; Roberts, D.; Hulmston, P. Drugs on money. *Anal. Chem.* **2000**, *72*, 397A-403A.
128. Pizzolato, T. M.; Lopez de Alda, M. J.; Barcelo, D. LC-based analysis of drugs of abuse and their metabolites in urine. *TrAC.* **2007**, *26*, 609-624.
129. Kraemer, T.; Paul, L. D. Bioanalytical procedures for determination of drugs of abuse in blood. *Anal. Bioanal. Chem.* **2007**, *388*, 1415-1435.
130. Srogi, K. Testing for drugs in hair – A review of chromatographic procedures. *Microchim. Acta.* **2006**, *154*, 191-212.
131. Boumba, V. A.; Ziavrou, K. S.; Vougiouklakis, T. Hair as a biological indicator of drug use, drug abuse or chronic exposure to environmental toxicants. *Int. J. Toxicol.* **2006**, *25*, 143-163.
132. Raharjo, T. J.; Verpoorte, R. Methods for the analysis of cannabinoids in biological materials: A review. *Phytochem. Anal.* **2004**, *15*, 79-94.
133. Lachenmeier, D. W.; Walch, S. G. Analysis and toxicological evaluation of cannabinoids in hemp food products – A review. *EJEAFChe.* **2005**, *4*, 812-826.
134. Hansen, S. H. Sample preparation and separation techniques for bioanalysis of morphine and related substances. *J. Sep. Sci.* **2009**, *32*, 825-834.
135. Wells, D. High throughput bioanalytical sample preparation. Methods and automation strategies., 1st ed.; Elsevier Science, Amsterdam, 2003.
136. Haapala, M.; Purcell, J. M.; Saarela, V.; Franssila, S.; Rodgers, R. P.; Hendrickson, C. L.; Kotiaho, T.; Marshall, A. G.; Kostiainen, R. Microchip atmospheric pressure photoionization for analysis of petroleum by fourier transform ion cyclotron resonance mass spectrometry. *Anal. Chem.* **2009**, *81*, 2799-2803.
137. Franssila, S.; Marttila, S.; Kolari, K.; Östman, P.; Kotiaho, T.; Kostiainen, R.; Lehtiniemi, R.; Fager, C.-M.; Manninen, J. A microfabricated nebulizer for liquid vaporization in chemical analysis. *JMEMS.* **2006**, *15*, 1251-1259.
138. Arulmozhiraja, S.; Fujii, T.; Morita, M. Density functional theory studies on radical ions of selected polychlorinated biphenyls. *J. Phys. Chem. A.* **2002**, *106*, 10590-10595.
139. Guprasad, N. P.; Haidar, N. A.; Manners, T. G. Applications of negative ion chemical ionization mass spectrometry technique in environmental analysis. *Commun. Soil Sci. Plant Anal.* **2002**, *33*, 3449-3456.
140. Lausevic, M.; Jiang, X.; Metcalfe, C. D.; March, R. E. Analysis of polychlorinated biphenyls by quadrupole ion trap mass spectrometry. Part II: Comparison of mass spectrometric detection using electron impact and selected-ion chemical ionization with electron capture detection. *Rapid Comm. Mass Spectrom.* **1995**, *9*, 927-936.
141. Arulmozhiraja, S.; Selvin, P. C.; Fujii, T. Structures, potential energy curves, and torsional barrier heights for selected polychlorinated biphenyls: A density functional theory study. *J. Phys. Chem. A.* **2002**, *106*, 1765-1769.

142. Parthasarathi, R.; Padmanabhan, J.; Subramanian, V.; Maiti, B.; Chattaraj, P. K. Chemical reactivity profiles of two selected polychlorinated biphenyls. *J. Phys. Chem. A.* **2003**, *107*, 10346-10352.
143. Trösken, E. R.; Straube, E.; Lutz, W. K.; Völkel, W.; Patten, C. Quantitation of lanosterol and its major metabolite FF-MAS in an inhibition assay of CYP51 by azoles with atmospheric pressure photoionization based LC-MS/MS. *J. Am. Soc. Mass Spectrom.* **2004**, *15*, 1216-1221.
144. van Leeuwen, S. M.; Hendriksen, L.; Karst, U. Determination of aldehydes and ketones using derivatization with 2,4-dinitrophenylhydrazine and liquid chromatography-atmospheric pressure photoionization-mass spectrometry. *J. Chromatogr. A.* **2004**, *1058*, 107-112.
145. Wang, G.; Hsieh, Y.; Korfmacher, W. A. Comparison of atmospheric pressure chemical ionization, electrospray ionization, and atmospheric pressure photoionization for the determination of cyclosporin A in rat plasma. *Anal. Chem.* **2005**, *77*, 541-548.
146. Kawano, S.; Murata, H.; Mikami, H.; Mukaibatake, K.; Waki, H. Method optimization for analysis of fullerenes by liquid chromatography/atmospheric pressure photoionization mass spectrometry. *Rapid Commun. Mass Spectrom.* **2006**, *20*, 2783-2785.
147. Chang, J.; Lawless, P. A.; Yamamoto, T. Corona discharge processes. *IEEE Trans. Plasma Sci.* **1991**, *19*, 1152-1166.
148. Thomson, B. A.; Sakuma, T.; Fulford, J.; Lane, D. A.; Reid, N. M. Fast *in situ* measurement on PCB levels in ambient air to ng m^3 levels using a mobile atmospheric pressure chemical ionization mass spectrometer system. *Adv. Mass Spectrom.* **1980**, *8B*, 1422-1428.
149. Yamada, M.; Suga, M.; Waki, I.; Sakamoto, M.; Morita, M. Continuous monitoring of polychlorinated biphenyls in air using direct samping APCI/ITMS. *Int. J. Mass Spectrom.* **2005**, *244*, 65-71.
150. World Anti-Doping Agency. Minimum required performance levels for detection of prohibited substance. http://www.Wada-Ama.org/rtecontent/document/ MINIMUM_REQUIRED_PERFORMANCE_LEVELS_TD_v1_0_January_2009. pdf, *accessed 18-03-2009*.
151. van Oeveren, A.; Motamedi, M.; Mani, N. S.; Marschke, K. B.; Lopez, F. J.; Schrader, W. T.; Negro-Vilar, A.; Zhi, L. Discovery of 6-N,N-bis(2,2,2-trifluoroethyl)amino-4-trifluoromethylquinolin-2(1H)-one as a novel selective androgen receptor modulator. *J. Med. Chem.* **2006**, *49*, 6143-6146.
152. van Oeveren, A.; Pio, B. A.; Tegley, C. M.; Higuchi, R. I.; Wu, M.; Jones, T. K.; Marschke, K. B.; Negro-Vilar, A.; Zhi, L. Discovery of an androgen receptor modulator pharmacophore based on 2-quinolinones. *Bioorg. Med. Chem. Lett.* **2007**, *17*, 1523-1526.
153. Pointet, K.; Milliet, A.; Hoyau, S.; Renou-Gonnord, M. F. Proton affinities of polybenzenoid aromatic hydrocarbons and those with five-membered rings. *J. Comput. Chem.* **1997**, *18*, 629-637.
154. Kauppila, T. J.; Talaty, N.; Salo, P. K.; Kotiaho, T.; Kostiainen, R.; Cooks, R. G. New surfaces for desorption electrospray ionization mass spectrometry: Porous silicon and ultra-thin layer chromatography plates. *Rapid Commun. Mass Spectrom.* **2006**, *20*, 2143-2150.
155. Kauppila, T. J.; Wiseman, J. M.; Ketola, R. A.; Kotiaho, T.; Cooks, R. G.; Kostiainen, R. Desorption electrospray ionization mass spectrometry for the analysis of pharmaceuticals and metabolites. *Rapid Commun. Mass Spectrom.* **2006**, *20*, 387-392.
156. Ifa, D. R.; Manicke, N. E.; Rusine, A. L.; Cooks, R. G. Quantitative analysis of small molecules by desorption electrospray ionization mass spectrometry from

polytetrafluoroethylene surfaces. *Rapid Commun. Mass Spectrom.* **2008**, *22*, 503-510.

157. Ulleras, E.; Ohlsson, A.; Oskarsson, A. Secretion of cortisol and aldosterone as a vulnerable target for adrenal endocrine disruption – Screening of 30 selected chemicals in the human H295R cell model. *J. Appl. Toxicol.* **2008**, *28*, 1045-1053.
158. Sergent, T.; Dupont, I.; Jassogne, C.; Ribonnet, L.; van der Heiden, E.; Scippo, M. L.; Muller, M.; McAlister, D.; Pussemier, L.; Larondelle, Y.; Schneider, Y. J. CYP1A1 induction and CYP3A4 inhibition by the fungicide imazalil in the human intestinal Caco-2 cells – Comparison with other conazole pesticides. *Toxicol. Lett.* **2009**, *184*, 159-168.
159. Harrison, R. M.; Smith, D. J. T.; Luhana, L. Source apportionment of atmospheric polycyclic aromatic hydrocarbons collected from an urban location in Birmingham, U.K. *Environ. Sci. Technol.* **1996**, *30*, 825.
160. Trapido, M. Polycyclic aromatic hydrocarbons in Estonian soil: Contamination and profiles. *Environ. Pollut.* **1999**, *105*, 67-74.
161. Masih, A.; Taneja, A. Polycyclic aromatic hydrocarbons (PAHs) concentrations and related carcinogenic potencies in soil at a semi-arid region of India. *Chemosphere.* **2006**, *65*, 449-456.
162. Talaty, N.; Mulligan, C. C.; Justes, D. R.; Jackson, A. U.; Noll, R. J.; Cooks, R. G. Fabric analysis by ambient mass spectrometry for explosives and drugs. *Analyst.* **2008**, *133*, 1532-1540.
163. Lurie, I. S.; Toske, S. G. Applicability of ultra-performance liquid chromatography-tandem mass spectrometry for heroin profiling. *J. Chromatogr. A.* **2008**, *1188*, 322-326.

Corrections to the original papers

Paper I

Page 430, caption to Table 3: Concentrations of selected PCBs in soil samples.